

Chiral Osmium Complexes with Sterically Bulky Schiff-Base Ligands. Crystal Structures of Os(IV) Derivatives and the Reactivity and Catalytic Cyclopropanation of Alkenes with EDA

Jing Zhang,[†] Jiang-Lin Liang,[†] Xian-Ru Sun,[†] Hai-Bing Zhou,[†] Nian-Yong Zhu,[†] Zhong-Yuan Zhou,[‡] Philip Wai Hong Chan,^{*,†} and Chi-Ming Che^{*,†}

Department of Chemistry and Open Laboratory of Chemical Biology of the Institute of Molecular Technology for Drug Discovery and Synthesis, The University of Hong Kong, Pokfulam Road, Hong Kong, P. R. China, and Department of Applied Biology and Chemical Technology, The Hong Kong Polytechnic University, Hung Hom, Kowloon, Hong Kong, P. R. China

Received December 22, 2004

The syntheses and reactivities of sterically encumbered *trans*-dioxoosmium(VI) complexes containing Schiff-base ligands bis(3,5-di-*tert*-butylsalicylidene)-1,2-cyclohexane-diamine (H₂Bu-salch) and bis(3,5-dibromosalicylidene)-1,2-cyclohexane-diamine (H₂Br-salch) are described. Reactions of [Os^{VI}(Bu-salch)O₂] (**1a**) and [Os^{VI}(Br-salch)O₂] (**1b**) with PPh₃, *p*-X-arylamines (X = NO₂, CN), N₂H₄·H₂O, Ph₂NNH₂, SOCl₂, CF₃CO₂H, Br₂, and I₂ under reducing conditions gave [Os^{IV}(Br-salch)(OPPh₃)₂] (**2**), [Os^{IV}(Br-salch)(*p*-X-C₆H₄NH)₂] (**3**), [*μ*-O-{Os^{IV}(Bu-salch)(*p*-NO₂C₆H₄NH)}₂] (**4**), [Os^{IV}(Br-salch)(N₂)(H₂O)] (**5**), [Os^{IV}(Bu-salch)(OH)(Cl)] (**6**), [Os^{IV}(Bu-salch)(OH)₂] (**7**), [Os^{IV}(Bu-salch)-Cl₂] (**8**), [Os^{IV}(Bu-salch)(CF₃CO₂)₂] (**9**), [Os^{IV}(Bu-salch)Br₂] (**10**), and [Os^{IV}(Bu-salch)I₂] (**11**), respectively. X-ray crystal structure determinations of [Os^{IV}(Br-salch)(*p*-NO₂C₆H₄NH)₂] (**3a**), [Os^{IV}(Br-salch)(*p*-CNC₆H₄NH)₂] (**3b**), **6**, **8**, **9**, and **11** reveal the Os–N(amido) distances to be 1.965(4)–1.995(1) Å for the bis(amido) complexes, Os–Cl distances of 2.333(8)–2.3495(1) Å for **6** and **8**, Os–O(CF₃CO₂) distances of 2.025(6)–2.041(6) Å for **9**, and Os–I distances of 2.6884(6)–2.6970(6) Å for **11**. Upon UV irradiation, (1*S*,2*S*)-(**1a**) reacted with aryl-substituted alkenes to give the corresponding epoxides in moderate yields, albeit with no enantioselectivity. The (1*R*,2*R*)-**6** catalyzed cyclopropanation of a series of substituted styrenes exhibited moderate to good enantioselectivity (up to 79% ee) and moderate *trans* selectivity.

Introduction

The chemistry of dioxoosmium(VI) complexes containing multianionic Schiff-base ligands has come under increasing scrutiny in recent years.^{1,2} Unlike their ruthenium counterparts, the greater stability of dioxoosmium(VI) Schiff-base

complexes has rendered them to be an invaluable model system for understanding the physical and spectroscopic properties of their ruthenium analogues, which should be more reactive toward organic transformations. Previous works by Che and co-workers had described a one-pot synthesis of *trans*-[Os^{VI}(salen)O₂] [salen = *N,N'*-bis(salicylidene)ethylenediamine] and the susceptibility of this complex to undergo reduction in the presence of PPh₃ and thiols.^{2a} In view of these works showing that dioxoruthenium-(VI) porphyrins are useful catalysts for a number of organic transformations,^{3,4} we were intrigued with the possibility of developing similar chemistry with ruthenium and osmium complexes containing inexpensive Schiff-base ligands. Indeed, chiral metal Schiff-base complexes have been demonstrated to be versatile catalysts for enantioselective organic transformation reactions. Pioneering work by Nakamura and co-workers showed that chiral (Schiff-base)cobalt(II) com-

* Authors to whom correspondence should be addressed. Fax: (852) 2857 1586. Tel: (852) 2859 2154. E-mail: cmche@hku.hk (C.-M.C.); pwhchan@hkuc.hku.hk (P.W.H.C.).

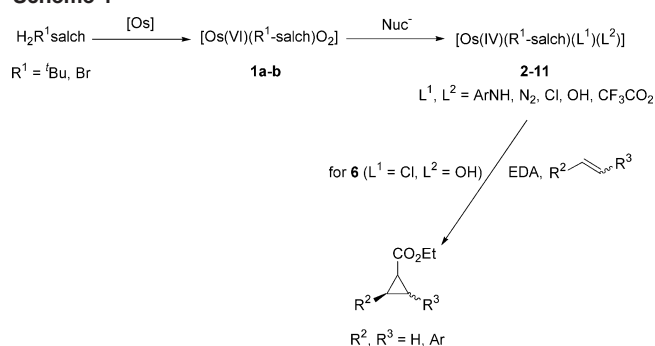
[†] The University of Hong Kong.

[‡] The Hong Kong Polytechnic University.

- (1) (a) Lay, P. A.; Harman, W. D. *Adv. Inorg. Chem.* **1991**, 37, 219. (b) Lynch, W. E.; Lintvedt, R. L.; Shui, X. Q. *Inorg. Chem.* **1991**, 30, 1014. (c) Wong, T.-W.; Lau, T.-C.; Wong, W.-T. *Inorg. Chem.* **1999**, 38, 6181.
- (2) (a) Che, C.-M.; Cheng, W.-K.; Mak, T. C. W. *Inorg. Chem.* **1986**, 25, 703. (b) Che, C.-M.; Cheng, W.-K.; Mak, T. C. W. *Inorg. Chem.* **1988**, 27, 250. (c) Cheng, W.-K.; Wong, K.-Y.; Tong, W.-F.; Lai, T.-F.; Che, C.-M. *J. Chem. Soc., Dalton Trans.* **1992**, 91. (d) Yip, K.-L.; Yu, W.-Y.; Chan, P.-M.; Zhu, N.-Y.; Che, C.-M. *J. Chem. Soc., Dalton Trans.* **2003**, 3556.

plexes are effective catalysts for asymmetric methylene transfer reactions.⁵ Jacobsen and Katsuki showed that chiral manganese(III) Schiff-base complexes catalyzed highly enantioselective alkene epoxidation and C–H bond oxidations.⁶ More recently, Katsuki et al. reported that Ru(II), Co(II), and Co(III) Schiff-base complexes catalyzed cyclopropanation of alkenes with good to high cis diastereo- and enantioselectivities.^{6c,7} The applications of chiral ruthenium(II) and manganese(III) Schiff-base complexes in stereoselective nitrene transfer reactions to C=C bonds and insertion to saturated C–H bonds have also been reported.^{6,8} Herein, we present the synthesis and characterization of *trans*-dioxoosmium(VI) complexes supported by the sterically encumbered chiral Schiff-base ligands bis(3,5-di-*tert*-butylsalicylidene)-1,2-cyclohexane-diamine (H₂/Bu-salch) and bis(3,5-dibromosalicylidene)-1,2-cyclohexane-diamine (H₂Br-salch) and the reactivities of these compounds toward PPh₃, amines, hydrazines, and nucleophiles under reducing conditions and alkenes under photolytic conditions. The *trans*-osmium(IV) Schiff-base complexes obtained from these reactions have been structurally characterized by X-ray

Scheme 1



crystallographic analysis. We also describe a chiral osmium(IV) Schiff-base-catalyzed protocol for alkene cyclopropanation with ethyl diazoacetate (EDA) that was accomplished with moderate *trans* selectivity and moderate to good enantioselectivities (Scheme 1).

Results and Discussion

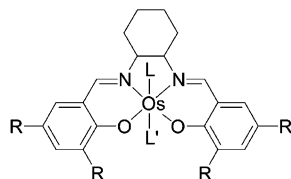
A. Dioxoosmium(VI) Schiff-Base Complexes [Os^{VI}(Bu-salch)O₂] (1a) and [Os^{VI}(Br-salch)O₂] (1b). i. Synthesis.

A number of first row transition metal complexes containing chelating multianionic ligands have been extensively studied for their catalytic activities in carbon–carbon, carbon–oxygen, and carbon–nitrogen bond formation reactions.^{6–8} This is in contrast to only a handful reports on the chemistry of late transition metal Schiff-base complexes. Previous works by us² and others^{1c,9} showed that certain [Os^{VI}(Schiff-base)O₂] complexes could be readily prepared by reacting the corresponding Schiff-base ligand with K₂[OsO₂(OH)₄]. However, a similar reaction of K₂[OsO₂(OH)₄] with either H₂/Bu-salch or H₂Br-salch failed to result in metal complexation. In this work, *trans*-dioxoosmium(VI) Schiff-base complexes **1a** and **1b** were prepared through a modification of the literature method.^{1c,2,9} Treatment of K₂[OsO₂(OH)₄] (0.27 mmol) with either H₂/Bu-salch or H₂Br-salch (0.27 mmol) in a solution of MeOH (25 mL) containing a few drops of HCl followed by treatment with 2,6-lutidine at room temperature gave **1a** and **1b** in yields of 70 and 65%, respectively (Figure 1). Under these conditions, (1*R*,2*R*)- and (1*S*,2*S*)-**1a** were also prepared from the reactions of K₂[OsO₂(OH)₄] with (1*R*,2*R*)- and (1*S*,2*S*)-H₂/Bu-salch. The enantiopurities of these two latter complexes were determined on the basis of circular dichroism spectroscopy ([ϕ]_{(1*R*,2*R*)-1a} + [ϕ]_{(1*S*,2*S*)-1a} ≈ 0).¹⁰ The addition of HCl was essential for the synthesis; presumably, proton was used to remove the strongly coordinated OH[−] group.

ii. Reactivity. Previous studies demonstrated that [Os^{VI}(14TMC)O₂]²⁺ (14TMC = 1,4,7,11-tetramethyl-1,4,7,11-cyclotetraazanonane) and [Os^{VI}(CN)₄O₂](Ph₄As)₂ are powerful photo-oxidants, undergoing light-induced oxygen atom transfer reactions with trialkylphosphines, dialkylsulfides, and alkenes.¹¹ In light of these works, we reasoned that similar

- (3) For works by us, see: (a) Leung, W. H.; Che, C.-M. *J. Am. Chem. Soc.* **1989**, *111*, 8812. (b) Ho, C.; Leung, W.-H.; Che, C.-M. *J. Chem. Soc., Dalton Trans.* **1991**, 2933. (c) Lai, T.-S.; Zhang, R.; Cheung, K.-K.; Kwong, H.-L.; Che, C.-M. *Chem. Commun.* **1998**, 1583. (d) Liu, C.-J.; Yu, W.-Y.; Peng, S.-M.; Mak, T. C. W.; Che, C.-M. *J. Chem. Soc., Dalton Trans.* **1998**, 1805. (e) Lai, T.-S.; Kwong, H.-L.; Zhang, R.; Che, C.-M. *J. Chem. Soc., Dalton Trans.* **1998**, 3559. (f) Liu, C.-J.; Yu, W.-Y.; Che, C.-M.; Yeung, C.-H. *J. Org. Chem.* **1999**, *64*, 7365. (g) Zhang, R.; Yu, W.-Y.; Lai, T.-S.; Che, C.-M. *Chem. Commun.* **1999**, 409; *Chem. Commun.* **1999**, 757. (h) Zhang, R.; Yu, W.-Y.; Lai, T.-S.; Che, C.-M. *Chem. Commun.* **1999**, 1791. (i) Zhang, R.; Yu, W.-Y.; Wong, K.-Y.; Che, C.-M. *J. Org. Chem.* **2001**, *66*, 8145. (j) Zhang, R.; Yu, W.-Y.; Sun, H.-Z.; Liu, W.-S.; Che, C.-M. *Chem.-Eur. J.* **2002**, *8*, 2495.
- (4) For works by others, see: (a) Groves, J. T.; Quinn, R. *Inorg. Chem.* **1984**, *23*, 3844. (b) Groves, J. T.; Quinn, R. *J. Am. Chem. Soc.* **1985**, *107*, 5790. (c) Groves, J. T.; Ahn, K. H. *Inorg. Chem.* **1987**, *26*, 3831. (d) Tavares, M.; Ramasseul, R.; Marchon, J. C. *Catal. Lett.* **1990**, *4*, 163. (e) Ohtake, H.; Higuchi, T.; Hirobe, M. *J. Am. Chem. Soc.* **1992**, *114*, 10660. (f) Tokita, Y.; Yamaguchi, K.; Watanabe, Y.; Morishima, I. *Inorg. Chem.* **1993**, *32*, 329. (g) Le Mau, P.; Bahri, H.; Simonneaux, G. *Chem. Commun.* **1994**, 1287. (h) Le Mau, P.; Bahri, H.; Simonneaux, G.; Toupet, L. *Inorg. Chem.* **1995**, *34*, 4691. (i) Morice, C.; Le Mau, P.; Simonneaux, G. *Tetrahedron Lett.* **1996**, *37*, 6701. (j) Bailey, A. J.; James, B. R. *Chem. Commun.* **1996**, 2343. (k) Gross, Z.; Ini, S. *J. Org. Chem.* **1997**, *62*, 5514. (l) Morice, C.; Le Mau, P.; Simonneaux, G.; Toupet, L. *J. Chem. Soc., Dalton Trans.* **1998**, 4165. (m) Morice, C.; Le Mau, P.; Moinet, C.; Simonneaux, G. *Inorg. Chim. Acta* **1998**, *273*, 142. (n) Gross, Z.; Ini, S. *Org. Lett.* **1999**, *1*, 2077. (o) Chen, C.-Y.; Cheng, S.-H.; Su, Y. O. *J. Electroanal. Chem.* **2000**, *487*, 51.
- (5) Nakamura, A.; Konisi, A.; Tatsuno, Y.; Otsuka, S. *J. Am. Chem. Soc.* **1978**, *100*, 3443.
- (6) (a) Müller, P. In *Advances in Catalytic Processes*; Doyle, M. P., Ed.; JAI Press: Greenwich, CT, 1997; Vol. 2, p 113. (b) Jacobsen, E. N.; Wu, M. H. In *Comprehensive Asymmetric Catalysis*; Jacobsen, E. N., Pfaltz, A., Yamamoto, H., Eds.; Springer: New York, 1999; p 607–649. (c) Katsuki, T. In *Catalytic Asymmetric Synthesis*, 2nd ed.; Ojima, I., Ed.; Wiley-VCH: New York, 2000; p 287.
- (7) (a) Fukuda, T.; Katsuki, T. *Tetrahedron* **1997**, *53*, 7201. (b) Uchida, T.; Irie, R.; Katsuki, T. *Tetrahedron* **2000**, *56*, 3501. (c) Niimi, T.; Uchida, T.; Irie, T.; Katsuki, T. *Tetrahedron Lett.* **2000**, *41*, 3647. (d) Uchida, T.; Saha, B.; Katsuki, T. *Tetrahedron Lett.* **2001**, *42*, 2521.
- (8) For recent reviews, see: (a) Müller, P.; Fruit, C. *Chem. Rev.* **2003**, *103*, 2905. (b) Katsuki, T. *Synlett* **2003**, 281. For recent examples, see: (c) Noda, K.; Hosoya, N.; Irie, R.; Ito, Y.; Katsuki, T. *Synlett* **1993**, 469. (d) Nishikori, H.; Katsuki, T. *Tetrahedron Lett.* **1996**, *37*, 9245. (e) Kohmura, Y.; Katsuki, T. *Tetrahedron Lett.* **2001**, *42*, 3339. (f) Liang, J.-L.; Yu, X.-Q.; Che, C.-M. *Chem. Commun.* **2002**, 124. (g) Omura, K.; Uchida, T.; Irie, R.; Katsuki, T. *Chem. Commun.* **2004**, 2060.

- (9) (a) Anson, F. C.; Collins, T. J.; Gipson, S. L.; Keech, J. T.; Krafft, T. E.; Peake, G. T. *J. Am. Chem. Soc.* **1986**, *108*, 6593. (b) Muller, J. G.; Takeuchi, K. *J. Inorg. Chem.* **1987**, *26*, 3634.
- (10) See the Supporting Information for circular dichroism spectra of (1*R*,2*R*)- and (1*S*,2*S*)-**1a**.



- 1a**, R = ^tBu, L = L' = O, [Os^{VI}(^tBu-salch)O₂];
1b, R = Br, L = L' = O, [Os^{VI}(Br-salch)O₂];
2, R = Br, L = L' = OPPh₃, [Os^{II}(Br-salch)(OPPh₃)₂];
3a, R = Br, L = L' = *p*-NO₂C₆H₄NH, [Os^{IV}(Br-salch)(*p*-NO₂C₆H₄NH)₂];
3b, R = Br, L = L' = *p*-CNC₆H₄NH, [Os^{IV}(Br-salch)(*p*-CNC₆H₄NH)₂];
4, R = ^tBu, L = *p*-NO₂C₆H₄NH, L' = [Os^{IV}(^tBu-salch)(L)]-O,
 [μ-O-{Os^{IV}(^tBu-salch)(*p*-NO₂C₆H₄NH)}₂];
5, R = Br, L = N₂, L' = H₂O, [Os^{II}(Br-salch)(N₂)(H₂O)];
6, R = ^tBu, L = Cl, L' = OH, [Os^{IV}(^tBu-salch)(OH)(Cl)];
7, R = ^tBu, L = L' = OH, [Os^{IV}(^tBu-salch)(OH)₂];
8, R = ^tBu, L = L' = Cl, [Os^{IV}(^tBu-salch)Cl₂];
9, R = ^tBu, L = L' = CF₃CO₂, [Os^{IV}(^tBu-salch)(CF₃CO₂)₂];
10, R = ^tBu, L = L' = Br, [Os^{IV}(^tBu-salch)Br₂];
11, R = ^tBu, L = L' = I, [Os^{IV}(^tBu-salch)I₂].

Figure 1. Dioxoosmium(VI) and osmium(IV) Schiff-base complexes prepared in this work.

Table 1. Light-Induced Oxidation of Alkenes with **1a**^a

Entry	Substrate	Epoxide	Yield (%) ^b	Benzaldehyde Yield (%)
1			23	28
2			26	14
3			15	22
4			27	- ^c

^a Reaction conditions: (1*S*,2*S*)-**1a**/alkene = 1:100; degassed 2:1 CH₂Cl₂/MeCN; UV irradiation for 24 h; analyzed by GC analysis. ^b Yield determined by GC analysis and based on the (1*S*,2*S*)-**1a** used. ^c Not detected.

reactivities could be observed for [Os^{VI}{(1*S*,2*S*)-(^tBu-salch)-O₂}] (**1a**) when it is subjected to UV irradiation (Table 1). Thus, when a degassed CH₂Cl₂/MeCN (2:1 v/v) solution containing 1 equiv of (1*S*,2*S*)-**1a** and 100 equiv of styrene was placed in a photochemical reactor (Rayonet RPR-100) and irradiated with an array of 16 low-pressure mercury arc lamps (RPR-2537) over a 24 h period, a color change from orange to green was observed. Analysis of the crude reaction mixture obtained after photolysis by fast atom bombardment (FAB) mass spectrometry revealed the presence of cluster peaks at *m/z* 737, 753, 767, 769, and 1522 that could be assigned to [Os(^tBu-salch)], [Os(^tBu-salch)O], **1a**, [Os(^tBu-salch)(OH)₂], and [Os(^tBu-salch)(O)₂O], respectively (see Figure S16 in the Supporting Information). In addition, the ν(OsO₂) stretch at 832 cm⁻¹ detected by IR spectroscopic analysis (see later section) disappeared, suggesting that the

dioxoosmium(VI) moiety was no longer present. Under these conditions, styrene oxide along with benzaldehyde were furnished in 23 and 28% yield, respectively, on the basis of gas chromatography (GC) analysis (Table 1, entry 1). However, the epoxidation of styrene was found to be non-enantioselective. Similar photochemical reactions with *cis*- and *trans*-β-methylstyrene and 1,2-dihydronaphthalene with (1*S*,2*S*)-**1a** gave the corresponding epoxidation products in moderate yields (Table 1, entries 2–4). The reaction of cyclooctene with (1*S*,2*S*)-**1a** gave no epoxidation product detected by either ¹H NMR or GC analysis.

In the absence of either UV irradiation or a reductant, neither [Os^{VI}(^tBu-salch)O₂] (**1a**) nor [Os^{VI}(Br-salch)O₂] (**1b**) was found to react with styrene, ethanol, 1,3-dimethylimidazolidine-2-thione, or aniline under a variety of conditions, such as at temperature up to 80 °C and with the use of excess reactants. In contrast, reaction of **1a** with 6 equiv of PPh₃ in MeCN at room temperature for 8 h gave a green solution. Analysis of the solution by FAB mass spectrometry revealed the presence of cluster peaks that could be assigned to [Os(^tBu-salch)(PPh₃)], [Os(^tBu-salch)(OPPh₃)(OH)], and [Os(^tBu-salch)(OPPh₃)(PPh₃)]. No [Os(^tBu-salch)-(MeCN)_{*m*}]^{*n*+} species were found. The analogous reaction of **1b** with 6 equiv of PPh₃ in MeCN at room temperature, on the other hand, furnished [Os^{II}(Br-salch)(OPPh₃)₂] (**2a**) as the sole product in 60% yield, and tentatively characterized on the basis of IR measurements and FAB mass spectrometry (see the Experimental Section).¹²

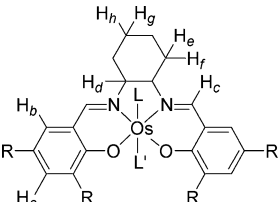
The bis(amido)osmium(IV) complexes [Os^{IV}(Br-salch)(*p*-NO₂C₆H₄NH)₂] (**3a**) and [Os^{IV}(Br-salch)(*p*-CNC₆H₄NH)₂] (**3b**) were obtained in 30% yields when **1b** was treated with 2 equiv of either *p*-nitro- or *p*-cyanoaniline in the presence of hydrazine hydrate. Under similar conditions, the analogous reaction of **1a** with *p*-nitroaniline, however, gave the dinuclear μ-oxo-bridged complex **4** in 50% yield. Complex **4**, [μ-O-{Os^{IV}(^tBu-salch)(*p*-NO₂C₆H₄NH)}₂], was characterized by elemental analyses and FAB mass spectrometry. While no reaction was found between **1a** and hydrazine hydrate in dimethylformamide (DMF), the reaction of hydrazine hydrate with **1b** in DMF gave the dinitrogen complex [Os^{II}(Br-salch)-(N₂)(H₂O)] (**5**) in 50% yield. Structural elucidation of **5** was based on elemental analyses and IR spectroscopy (see later section).¹³ With diphenylhydrazine hydrochloride, [Os^{IV}(^tBu-salch)(OH)(Cl)] (**6**) was preferentially furnished in 80% yield, and no mono- or bis(hydrazido)osmium(IV) complex could be detected by either ¹H NMR spectroscopy or mass spectrometry. This is different from the analogous reaction of [Os-(Por)O₂] with diphenylhydrazine.¹⁴ [Os^{IV}{1*R*,2*R*}-(^tBu-salch)-(OH)(Cl)] (**6**) was similarly obtained from the reaction of diphenylhydrazine hydrochloride with [Os^{VI}{1*R*,2*R*}-(^tBu-salch)O₂] (**1a**). Repetition of this reaction with Et₃N to re-

(11) (a) Che, C.-M.; Yam, V. W. W.; Tang, W.-T. *Chem. Commun.* **1988**, 100. (b) Yam, V. W. W.; Che, C.-M. *New J. Chem.* **1989**, 13, 707. (c) Yam, V. W. W.; Che, C.-M. *Coord. Chem. Rev.* **1990**, 97, 93.

(12) Che, C.-M.; Lai, T.-F.; Chung, W.-C.; Schaefer, W. P.; Gray H. B. *Inorg. Chem.* **1987**, 26, 3907.

(13) (a) Albertin, G.; Antoniutti, S.; Baldan, D.; Bordignon, E. *Inorg. Chem.* **1995**, 34, 6205. (b) Li, Z. Y.; Huang J.-S.; Chan, M. C.-W.; Cheung, K.-K.; Che, C.-M. *Inorg. Chem.* **1997**, 36, 3064. (c) Coia, G. M.; Devenney, M.; White, P. S.; Meyer, T. J.; Wink, D. A. *Inorg. Chem.* **1997**, 36, 2341.

(14) Leung, S. K.-Y.; Huang J.-S.; Zhu, N.-Y.; Cheung, K.-K.; Che, C.-M. *Inorg. Chem.* **2003**, 42, 7266.

Table 2. ^1H NMR Spectra of **1a**, **3a**, **3b**, and **6–11**


complex	H _a signal (d, 2H)	H _b signal (d, 2H)	H _c signal (s, 2H)	H _d signal (m, 2H)	H _e –H _h signal (m, 8H)	^t Bu (4 × s, 32H) ^a	<i>p</i> -X–C ₆ H ₄ NH (m, 8H)
1a	7.14	7.66	8.38	3.98	3.81, 2.04, 1.73, 1.48	1.32, 1.58	
3a	7.53	7.86	9.38	3.92	2.24–0.86		8.02, 6.92 ^a
3b	7.52	7.77	9.23	4.00	3.31, 2.19, 1.68		7.46, 7.08 ^b
6	6.99, 6.81	10.58, 10.37	9.38, 8.30	2.86, 2.61	1.27, 0.85	2.32, 2.29, 0.57, 0.39	
7	6.41	8.30	5.35	3.17	1.69, 1.12, –0.07	1.91, 1.28	
8	8.04	12.43	16.44	4.94	1.99, 0.15, –1.27	2.37, –0.21	
9	7.56	10.40	14.07	6.31	2.31, 0.70, 0.42, –0.01	1.96, 0.34	
10	8.44	13.07	19.31	6.49	2.00, 0.08, –0.27, –1.49	2.46, –0.27	
11	8.82	13.73	22.15	8.35	2.00, 1.49, 0.31, –1.89	2.56, 0.31	

^a X = NO₂. ^b X = CN.

place KOH preferentially gave [Os^{IV}(^tBu-salch)(OH)₂] (**7**) in 60% yield. Thus, the role of diphenylhydrazine in these reactions could be that of a reductant. The reaction of [Os^{VI}(^tBu-salch)O₂] (**1a**) with either SOCl₂ or CF₃CO₂H under reducing conditions (i.e., N₂H₄·H₂O and PPh₃, respectively), on the other hand, afforded [Os^{IV}(^tBu-salch)Cl₂] (**8**) and [Os^{IV}(^tBu-salch)(CF₃CO₂)₂] (**9**) in 70 and 40% yield, respectively. Similarly, the analogous reaction of **1a** with either Br₂ or I₂ in the presence of N₂H₄·H₂O gave [Os^{IV}(^tBu-salch)Br₂] (**10**) and [Os^{IV}(^tBu-salch)I₂] (**11**) in 50 and 80% yield, respectively (Figure 1).

Under alkylating conditions, the reaction of **8** with either MeLi or PhLi was found to result in the formation of an amorphous brown solid. Although analysis of the reaction mixtures by conventional spectroscopic means was unable to elucidate the product(s) obtained, the detection of no stretching frequencies that could be assigned to the Schiff-base ligand by IR spectroscopy suggests that demetalation had occurred during the course of these reactions.

iii. Characterization. Complexes **1–11** are stable in the solid state and in solution. Exposure of a CDCl₃ solution containing **7**, for example, to air at room temperature for 1 month was found to result in no noticeable decomposition on the basis of ^1H NMR spectroscopic analysis.

The ^1H NMR spectra of **1a**, **3a**, **3b**, and **6–11** exhibit well-resolved signals at normal fields. This is consistent with the diamagnetic nature of related dioxoosmium(VI) and osmium(IV) Schiff-base complexes reported in the literature.^{2a–c} The spectral data are summarized in Table 2. The insolubility of **1b** and **5** in various deuterated solvents renders characterization of these complexes by NMR and UV–vis spectroscopy difficult.

The ^1H NMR spectrum of **1a** in CDCl₃ features the azomethine and ArCH protons shifted downfield to 8.38, 7.66, and 7.14 ppm relative to the respective signals of the free Schiff-base ligand at 7.29, 6.80, and 7.30 ppm, which is assignable to a deshielding effect by the axial oxo ligands (see the Supporting Information). A similar effect on the bridging methylene protons in **1a** causes an observed shift

of these signals to 3.95–3.98 ppm relative to those of the free ligand which are located in the 3.30–3.33 ppm region. This is comparable to the data noted for [Os^{VI}(R-salen)O₂] and [Os^{VI}(R-saltmen)O₂] {R = ^tPr, ^tBu, (3-Me)Bu; H₂-(saltmen) = *N,N'*-(1,1,2,2-tetramethylethylene)bis(salicylideneamine)}.^{2b} A marked downfield shift of the equatorial and axial CH protons of the cyclohexane ring in **1a** to 2.03–2.17 and 2.78–2.83 ppm, respectively, has also been observed. In the free ligand, these signals appear as a multiplet at 1.41–1.95 ppm. For **1a**, **3a**, **3b**, and **7–11**, where the axial ligands are equivalent, only one set of signals corresponding to the two azomethine, four ArCH, and four ^tBu groups is observed. For **6** with different axial ligands, a total of 10 signals for the 2 azomethine, 8 ArCH protons, and 4 ^tBu groups of the Schiff-base ligand are found (Figure 2). As depicted in Table 2, the chemical shift of the azomethine H_c protons shifts upfield by 0.15 ppm from **3a** to **3b**. This upfield shift is attributed to the strong electron-withdrawing effect of the NO₂ substituent in **3a**. A similar trend of the chemical shift of H_c from **6** to **8** has also been found. Replacing an axial Cl ligand in **8** with a OH ligand, as in **6**, results in an upfield shift of the H_c signal by > 7.0 ppm. A further upfield shift of the H_c signal to 5.35 ppm is observed when the Cl ligand in **6** (H_c signal = 8.30 and 9.38 ppm) is further replaced by another OH ligand, as in **7**.

An inspection of the ^1H NMR data of [Os^{IV}(^tBu-salch)-X₂] (**8**, X = Cl; **9**, X = CO₂CF₃; **10**, X = Br; **11**, X = I), listed in Table 2, shows a significant downfield shift of the Schiff-base ligand proton signals on going from **9** → **8** → **10** → **11**. This trend apparently correlates to the π -bonding interaction of the axial halide ligands with Os(IV), which would be most pronounced for the soft iodide ligand. The $d_{\pi}\{\text{Os(IV)}\}-p_{\pi}(\text{X}^-)$ interaction would compete with the π -bonding interaction between Os(IV) and the coordinated Schiff-base ligand and, hence, affecting the ring current-deshielding effect. Similar trends have also been reported in NMR studies on the Schiff-base^{2a,c–d} and porphyrinato¹⁵ complexes of ruthenium and osmium.

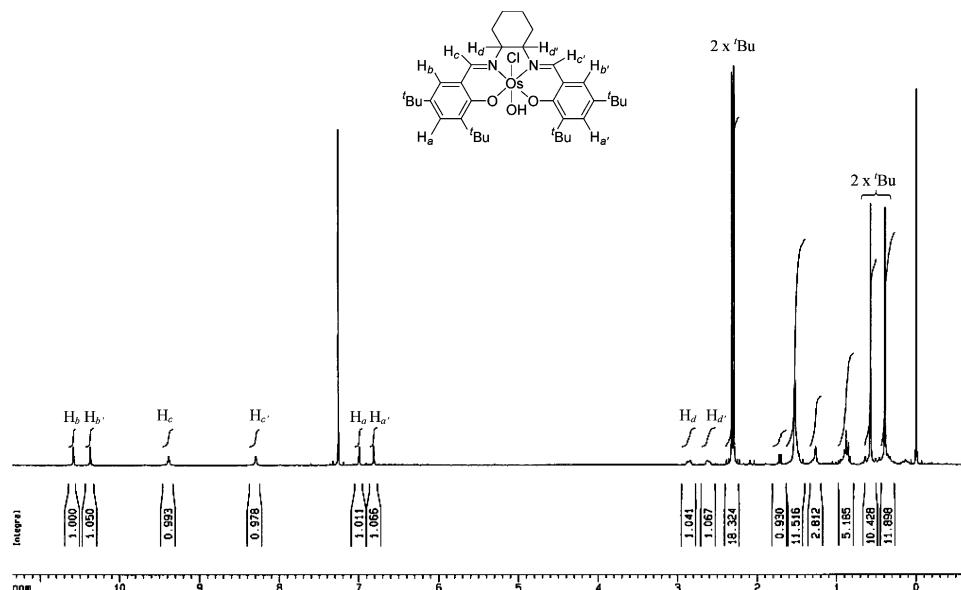


Figure 2. ^1H NMR spectrum of **6** in CDCl_3 .

Table 3. UV–Vis Spectral Data of **1a**, **2**, **3a**, **3b**, and **4–11** in CH_2Cl_2

complex	$\lambda_{\text{max}}/\text{nm}$ ($\log \epsilon/\text{dm}^3 \text{mol}^{-1} \text{cm}^{-1}$)
1a	272(4.17), 307(4.04), 377(3.72), 437(3.48)
2	356(4.17), 432(4.27)
3a	378(4.22), 653(4.23)
3b	390(4.00), 634(4.10)
4	384(4.75), 409(4.73), 463(4.57)
5	349(4.07), 399(4.10)
6	269(4.48), 347(4.14), 398(4.35), 702(4.00)
7	268(4.43), 370(4.33), 425(4.40), 594(3.76)
8	270(4.44), 310(4.08), 343(4.05), 406(4.28), 760(4.08)
9	233(4.47), 265(4.32), 338(3.96), 392(4.22), 756(4.00)
10	270(4.36), 327(4.01), 348(4.00), 411(4.27), 788(4.04)
11	271(4.45), 345(4.19), 414(4.48), 854(4.11)

The UV–vis data of **1a**, and **2–11** are summarized in Table 3. The UV–vis spectrum of **1a** (see Figure S4 in the Supporting Information) shows absorption bands at 272, 307, and 377 nm and a shoulder at 437 nm. The high energy bands at 272 and 307 nm, with respective $\log \epsilon$ values of 4.17 and 4.04 $\text{dm}^3 \text{mol}^{-1} \text{cm}^{-1}$, are dominated by intraligand charge-transfer transitions of the coordinated Schiff-base ligands, although the spin-allowed $p_\pi(\text{O}^{2-}) \rightarrow \text{Os}(\text{VI})$ charge-transfer transition of related *trans*-dioxoosmium(VI) complexes was reported to occur at a similar spectral region (ca. 300 nm).^{2b,16} Complexes **3a**, **3b**, and **6–11** exhibit a low energy band with λ_{max} lying between 594 and 854 nm. The λ_{max} value red-shifts by 2535 cm^{-1} on going from **6** to **8** and to **11** (Figures S5–S6 in the Supporting Information). We attribute this low energy absorption band as $p_\pi(\text{phenolate}) \rightarrow \text{Os}(\text{IV})$ with $p_\pi(\text{axial ligand}) \rightarrow \text{Os}(\text{IV})$ charge-transfer character.

Cyclic voltammetry was used to examine the redox properties of **1a**, **2**, **3a**, **3b**, and **6–11** in CH_2Cl_2 . The

Table 4. Electrochemical Data for the Osmium Schiff-Base Complexes **1a**, **3a**, **3b**, and **6–11** in CH_2Cl_2

complex	potential (V) ^a	
	oxidation	first reduction
1a	0.78, ^b 1.14 ^b	−1.39 ^b
3a	0.57, ^c 1.21 ^c	−0.89 ^b
3b	0.41, ^b 1.00 ^c	−1.09 ^b
6 ^d	0.51, ^c 0.85, ^c 1.05 ^c	−1.00 ^e
7 ^d	0.17, ^c 0.71, ^c 1.06 ^c	−1.33 ^e
8	0.75, ^e 1.50 ^c	−0.77 ^e
9	0.89, ^e 1.53 ^c	−0.64 ^e
10	0.73, ^e 1.49 ^c	−0.74 ^e
11	0.69, ^e 1.22 ^c	−0.72 ^e

^a Versus that of the $\text{Cp}_2\text{Fe}^{+/0}$ couple. ^b Quasi-reversible. ^c Irreversible. ^d Several irreversible oxidation waves are observed. ^e Reversible.

electrochemical data (vs $\text{Cp}_2\text{Fe}^{+/0}$ couple) for these complexes are tabulated in Table 4. The cyclic voltammogram of **1a**, shown in Figure 3, reveals two quasi-reversible oxidation waves and a quasi-reversible reduction wave. The reduction wave at −1.39 V is assigned to the reduction of $\text{Os}(\text{VI})$ to $\text{Os}(\text{V})$. The quasi-reversible oxidation couples of **1a** at 0.78 and 1.14 V are interesting because related dioxoosmium(VI) Schiff-base complexes were found to show irreversible oxidation at potentials 0.92–0.95 V.^{2b} The two oxidation couples of **1a** are attributed to ligand-centered oxidation because reversible oxidation couples with $E_{1/2}$ values of 0.69–0.89 V have also been found for the related $\text{Os}(\text{IV})$ complexes $[\text{Os}^{\text{IV}}(\text{Bu-salch})\text{X}_2]$ (**8**, $\text{X} = \text{Cl}$; **9**, $\text{X} = \text{CO}_2\text{CF}_3$; **10**, $\text{X} = \text{Br}$; **11**, $\text{X} = \text{I}$). The cyclic voltammograms of **8–11** also reveal an irreversible oxidation wave at E_{pa} values ranging from 1.22 to 1.53 V (see the Supporting Information). The potentials for the first and second oxidations of **8–11** are more anodic than those for the related $[\text{Os}^{\text{IV}}(\text{salen})(\text{OR})_2]$ ($\text{R} = \text{Me}, \text{Et}, \text{Pr}$) complexes (0.36–0.50 V).^{2c} In addition, the $E_{1/2}$ for the first oxidation couple becomes less anodic along the sequence **9** → **8** → **10** → **11**.

- (15) (a) Huang, J.-S.; Leung, S. K.-Y.; Cheung, K.-K.; Che, C.-M. *Chem.—Eur. J.* **2000**, *6*, 2971. (b) Li, Y.; Huang, J.-S.; Xu, G.-B.; Zhu, N.; Zhou, Z.-Y.; Che, C.-M.; Wong, K.-Y. *Chem.—Eur. J.* **2004**, *10*, 3486.
(16) Miskowski, V. M.; Gray, H. B.; Hopkins, M. D. *Adv. Transition Met. Coord. Chem.* **1996**, *1*, 159 and references therein.

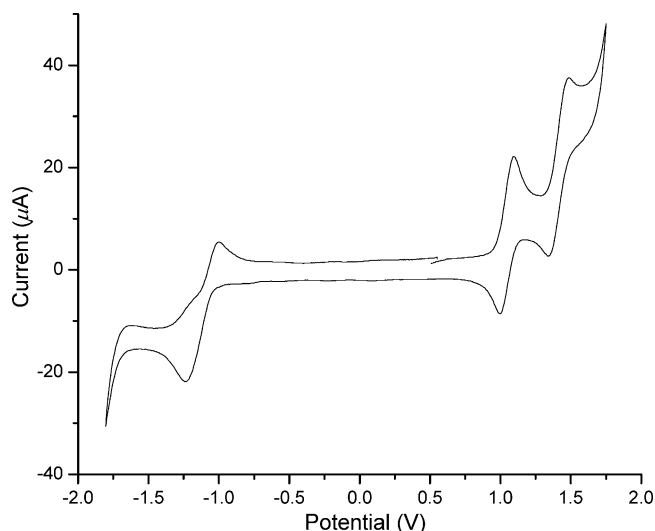


Figure 3. Cyclic voltammogram trace of **1a**, in CH_2Cl_2 at 298 K with 0.1 M $(\text{Bu}_4\text{N})\text{PF}_6$ as a supporting electrolyte (scan rate = 100 mVs^{-1} ; $\text{Cp}_2\text{Fe}^{+/-}$ = 0.27 V; working electrode = pyrolytic graphite).

This trend of $E_{1/2}$ values is in accord with a decrease in the inductive effect of the axial ligands, which follow the order $\text{CF}_3\text{CO}_2 > \text{Cl} > \text{Br} > \text{I}$. In contrast, the cyclic voltammograms of **3a** and **3b** revealed an irreversible oxidation peak with E_{pa} at 0.57 and 0.41 V for **3a** and **3b**, respectively. The irreversibility could be due to the electrochemical generation of an $\text{Os(V)}-\text{N}$ (amido) complex. Similarly, for **6** and **7**, several irreversible oxidation peaks in the 0.30–1.33 V region are found, which we tentatively assign to the oxidative deprotonation of the $\text{Os(IV)}-\text{OH}$ moiety.

The cyclic voltammograms of **3a**, **3b**, and **6–11** also show a reversible/quasi-reversible $\text{Os(IV)}/\text{Os(III)}$ couple at $E_{1/2}$ ranging from -0.49 to -1.33 V. A comparison of the electrochemical data revealed that the $E_{1/2}$ of $\text{Os(IV)}/\text{Os(III)}$ couples follow the trend $9 > 8, 10, 11 > 6 > 7$, which parallels the increase in π -donor strength of the axial ligands. As OH^- ligand is a strong σ - and π -donor, the Os(IV) site would be more electron rich because of strong $p\pi(\text{OH}^-)-d\pi\{\text{Os(IV)}\}$ π -bonding interaction. The axial halide ligands have little effect on the $E_{1/2}$ of $\text{Os(IV)}/\text{Os(III)}$ couple.

IR spectroscopic measurements of **1a** and **1b** reveal a $\nu_{\text{as}}(\text{OsO}_2)$ stretch at 833 cm^{-1} for **1a** and one at 841 cm^{-1} for **1b**. In both **1a** and **1b**, the absence of a $\nu(\text{OH})$ stretch indicates that the phenolic OH groups of the H_2salch ligand are deprotonated. Bands at ca. 1640 and 1560 cm^{-1} are assigned to $\nu(\text{C}=\text{N})$ and $\nu(\text{CO})$, respectively. For **2**, peaks at 1420 , 1155 , and 1066 cm^{-1} , assignable to $\nu(\text{P}-\text{Ph})$, and at 1121 cm^{-1} , assignable to $\nu(\text{P}=\text{O})$, are consistent with the stretching frequencies of the axial OPPh_3 ligands. The IR spectra of **3a–c** and **4** exhibit one sharp and three medium NH stretching bands at 3290 , 3296 , 3329 , and 3278 cm^{-1} , respectively. These stretching frequencies are higher than that observed for $[\text{Os}(\text{TPP})(\text{PhNH})_2]$ [$\text{H}_2(\text{TPP}) = \text{meso-tetrakis(phenyl)porphyrin}$] at 3253 cm^{-1} ¹³ but lower than that for $[\text{Os}(\text{Tp})(\text{NHPh})(\text{Cl})_2]$ [$\text{Tp} = \text{hydro-tris(1-pyrazolyl)-borate}$] at 3519 cm^{-1} .¹⁷ The IR spectrum of **5** reveals a band at 2017 cm^{-1} attributed to the $\nu(\text{N}_2)$ stretch.¹³ For **6** and **7**, sharp medium bands located at 3533 and 3557 cm^{-1} are

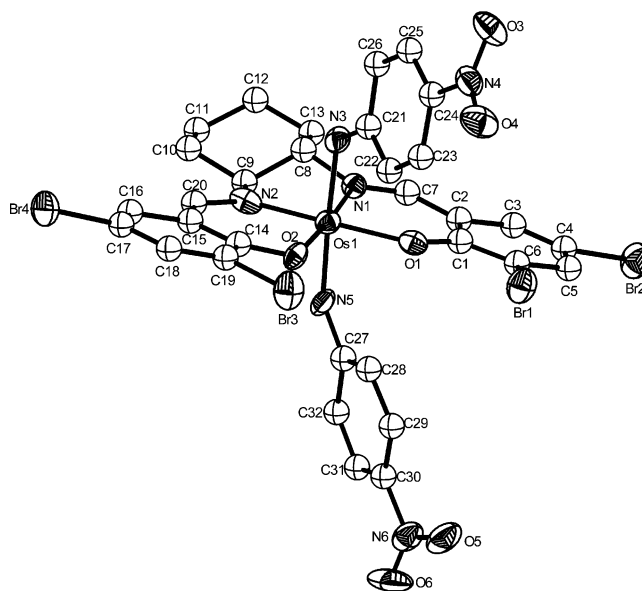


Figure 4. Perspective view of **3a**. Hydrogen atoms and solvent molecules have been omitted for clarity. Selected bond lengths (Å) and angles (deg): $\text{Os}-\text{O}(1)$ 2.005(9), $\text{Os}-\text{O}(2)$ 2.033(7), $\text{Os}-\text{N}(1)$ 2.025(9), $\text{Os}-\text{N}(2)$ 1.968(11), $\text{Os}-\text{N}(3)$ 1.995(10), $\text{Os}-\text{N}(5)$ 1.979(10), $\text{N}(1)-\text{C}(7)$ 1.28(14), $\text{N}(2)-\text{C}(9)$ 1.498(18), $\text{O}(1)-\text{Os}-\text{N}(1)$ 94.0(4), $\text{N}(2)-\text{Os}-\text{N}(3)$ 91.9(4), $\text{N}(2)-\text{Os}-\text{N}(5)$ 90.0(4), $\text{N}(3)-\text{Os}-\text{O}(1)$ 89.1(4), $\text{N}(3)-\text{Os}-\text{O}(2)$ 90.2(3), $\text{N}(3)-\text{Os}-\text{N}(1)$ 89.6(4), $\text{N}(5)-\text{Os}-\text{N}(1)$ 88.0(4), $\text{C}(21)-\text{N}(3)-\text{Os}$ 126.1(8), $\text{C}(27)-\text{N}(5)-\text{Os}$ 128.8(9).¹⁸

assigned to the $\nu(\text{OH})$ stretch. The positive ion FAB spectra of **1a** and **1b** each exhibit three signals that can be attributed to the parent ion $[\text{M}]^+$ and the $[\text{M} - \text{O}]^+$ and $[\text{M} - 2\text{O}]^+$ fragments. For **2–11**, the positive ion FAB spectra of these complexes revealed ion clusters assignable to the parent ion $[\text{M}]^+$ and the $[\text{M} - (\text{axial ligand})_n]^+$ fragments.

B. Structures of 3a, 3b, 6, 8, 9, and 11.¹⁸ Complexes **3a** and **3b** were recrystallized from $\text{CHCl}_3/\text{acetone}$, whereas **6**, **8**, and **9** were recrystallized from n -hexane/ CHCl_3 , and **11** was recrystallized from $\text{Et}_2\text{O}/\text{CH}_2\text{Cl}_2$ at room temperature. Perspective views of **3a–b**, **6**, **8**, **9** and **11** are depicted in Figures 4–9. The crystal data and structural refinements are given in Table 5.¹⁸

As shown in Figures 4 and 5, the axial ligands of **3a** and **3b** adopt a configuration where the aryl rings of the axial ligands are situated away from the cyclohexane ring, presumably to minimize unfavorable steric interactions with the Schiff-base ligand. The aromatic rings of the axial ligands sit in planes that are nearly perpendicular to the plane of the Schiff-base ligand, with dihedral angles between these planes equal to 80.4 and 85.1° for **3a** and 85.3 and 88.5° for **3b**. The amido aryl rings in these complexes are also located in the same plane with respect to each other, with dihedral angles between the planes occupied by the aryl rings of the amido ligands equal to 14.5° in **3a** and 4° in **3b**. The structures of **6**, **8**, and **11**, depicted in Figures 6, 7, and 9,

(17) Crevier, T. J.; Bennett, B. K.; Soper, J. D.; Bowman, J. A.; Dehestani, A.; Hrovat, D. A.; Lovell, S.; Kaminsky, W.; Mayer, J. M. *J. Am. Chem. Soc.* **2001**, *123*, 1059.

(18) CCDC 228404–228408 and 254698 contain the supplementary crystallographic data for this paper. These data can be obtained free of charge via www.ccdc.cam.ac.uk/conts/retrieving.html (or from the CCDC, 12 Union Road, Cambridge CB2 1EZ, UK. Fax: +44 1223 336033. E-mail: deposit@ccdc.cam.ac.uk).

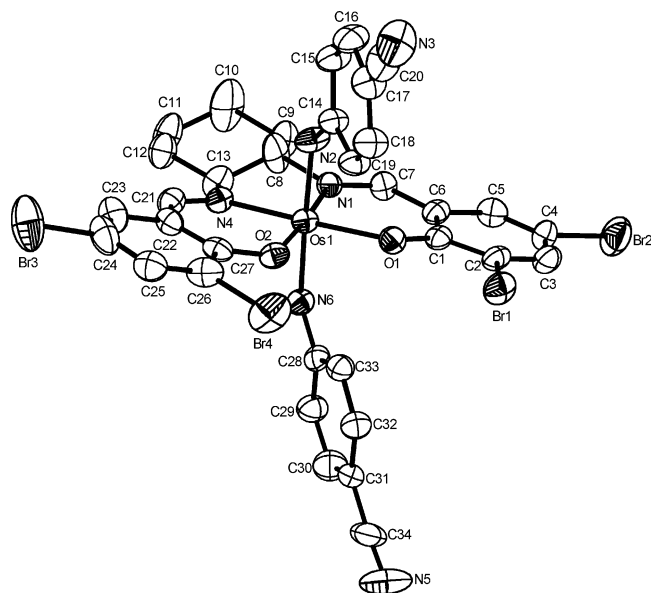


Figure 5. Perspective view of **3b**. Hydrogen atoms and solvent molecules have been omitted for clarity. Selected bond lengths (Å) and angles (deg): Os–O(1) 2.039(4), Os–O(2) 2.021(3), Os–N(1) 2.005(5), Os–N(2) 1.965(4), Os–N(4) 2.021(4), Os–N(6) 1.975(4), N(1)–C(7) 1.29(7), N(1)–Os–N(2) 89.8(2), N(2)–Os–O(1) 89.9(2), N(2)–Os–N(4) 90.1(2), N(4)–Os–O(1) 177.2(1), N(4)–Os–O(2) 92.7(2), N(6)–Os–O(2) 90.7(1), N(6)–Os–N(1) 89.5(1), C(14)–N(2)–Os(1) 132.1(4), C(28)–N(6)–Os(1) 130.8(4).¹⁸

respectively, reveal that the axial ligands, which are sterically less demanding than those of the arylamido groups of **3a** and **3b**, are also situated in planes that are at near right angles to the plane of the Schiff-base ligand. The average axial ligand–Os–N (imine) angle is between 86 and 94° in **6**, 89 and 92° in **8**, and 87 and 90° in **11**. The axial Cl and OH ligands in **6** are disordered. A perspective view of **9** is depicted in Figure 8. The plane occupied by the two CF₃CO₂ axial ligands is slightly tilted by ca. 10° from the idealized perpendicular plane with respect to the plane of the Schiff-base ligand. Presumably, in this conformation, any unfavorable steric interactions between the CF₃CO₂ axial ligands and the Schiff-base ligand are kept to a minimum. Ligand chelation in **3a**, **3b**, **6**, **8**, **9**, and **11** is found to result in a minimal distortion of the Os atom from the calculated least-squares plane of the Schiff-base ligand, with the metal in each complex sitting in the plane of the ligand. For each complex, the five-membered chelate ring comprising Os, the two N (imine) atoms, and the bridging C (cyclohexane) atoms sit in a gauche form, so that the two vicinal C atoms bonded to the bridging C (cyclohexane) are staggered with respect to each other.

The average Os–N (amido) distances in **3a** and **3b** are 1.987 and 1.97 Å, respectively. These distances are slightly longer than that found in [Os^{IV}(Tp)(NHPh)(Cl)₂] [1.919(6) Å],¹⁷ though similar to that of the Ru–NHAr bond [1.956(7) Å] in [Ru^{IV}(TTP)(*p*-Cl–PhNH)₂] [H₂(TTP) = *meso*-tetrakis(tolyl)porphyrin].¹⁹ The Os–N (amido) distances in **3a** and **3b** are also longer than the Os–N (imido) distance of 1.775 Å in [Os^{VI}(4-Cl–TPP)(N^tBu)₂]^{13b} [H₂(4-Cl–TPP) =

meso-tetrakis(*p*-chlorophenyl)porphyrin] and 1.749(7) Å in [Os^V(Tp)(Cl)₂(NH)].²⁰ They are, however, shorter than the Os–N (amido) distance in [Os₃(μ-dan)(CO)₁₀] [2.165 Å; H₂-(dan) = 1,8-diaminonaphthalene].²¹ The average Os–Cl distances in **6** and **8** [2.333(8)–2.349(1) Å] are similar, but they are slightly shorter than related values in [Os^{IV}(NPPH₃)-(salophen)(Cl)] [H₂(salophen) = *N,N'*-bis(salicylidene)-*o*-phenylenediamine; 2.424(5) Å]^{1c} and [Os(bpb)(PPh₃)(Cl)] [H₂-(bpb) = *N,N'*-bis(2'-pyridinecarboxamide)-1,2-benzene; 2.410(4) Å].²² The Os–OH distance of **6** is 1.94(2) Å, which is comparable to that for Os–O(OⁱPr) in [Os^{IV}(salen)(OⁱPr)₂] [1.92(3) Å].^{2c} In **9**, the average Os–O(CF₃CO₂) distance is 2.033 Å, which is longer than that in **6**. The bond angles between the axial ligands in **8** and **11** are 179 and 177°, respectively, which are close to the 180° value required for linearity. In comparison, the analogous angles between the two axial ligands in **6** and **9** are 170 and 167°, respectively, suggesting the Os-axial ligand moieties in these complexes to be slightly bent.

At this juncture, it is worthy to highlight that the crystal structures of **3a**, **3b**, **8**, **9**, and **11** not only show the chirality of the bonding environment around the osmium atom, but they also conform to an idealized *C*₂ molecular geometry with a pseudo-2-fold axis passing through the metal center and the midpoint of the bridging cyclohexane bond. In **6**, the axial ligands are different, consistent with ¹H NMR analysis of this complex.

C. [Os^{IV}{(1*R*,2*R*)-(Bu-salch)(OH)(Cl)}] (6**) Catalyzed Organic Reactions.** In the literature, Schiff-base complexes of Cr(V)²³ and Mn(III)^{12,24} are known to catalyze C–O bond formation reactions. Jacobsen and co-workers showed that [Mn^{III}{1*S*,2*S*}(Bu-salch)Cl]⁺ catalyzed the epoxidation of alkenes with enantioselectivities of up to 98% ee.²⁴ In this work, when (1*R*,2*R*)-**6** (2 mol %) was treated with a CH₂Cl₂ solution containing 1 equiv of styrene and 1.5 equiv of PhI=O, no epoxidation was found on the basis of GC analysis. Similarly, no aziridination product was detected by either ¹H NMR spectroscopy or GC analysis for the reaction of (1*R*,2*R*)-**6** (2 mol %) with 1 equiv of styrene and 1.5 equiv of PhI=NTs. In contrast, when 1.5 equiv of EDA was slowly added dropwise to a CH₂Cl₂ solution containing styrene (1 equiv) and (1*R*,2*R*)-**6** (1 mol %) at room temperature, 2-phenyl-cyclopropanecarboxylic acid ethyl ester was furnished in 50% yield and with a trans/cis ratio of 2.1:1.²⁵ On the basis of high-performance liquid chromatography (HPLC)

(19) Huang, J.-S.; Sun, X.-R.; Leung, S. K.-Y.; Cheung, K.-K.; Che, C.-M. *Chem.-Eur. J.* **2000**, *6*, 334.

(20) Huynh, M. H. V.; White, P. S.; John, K. D.; Meyer, T. J. *Angew. Chem., Int. Ed.* **2001**, *40*, 4049.
(21) Cabeza, J. A.; Noth, H.; Rosales-Hoz, M. D. J.; Sanchez-Cabrera, G. *Eur. J. Inorg. Chem.* **2000**, 2327.
(22) Che, C.-M.; Cheng, W.-K.; Mak, T. C. W. *Chem. Commun.* **1986**, 200.
(23) O'Mahony, C. P.; McGarrigle, E. M.; Renehan, M. F.; Ryan, K. M.; Kerrigan, N. J.; Bousquet, C.; Gilheany, D. G. *Org. Lett.* **2001**, *3*, 3435.
(24) (a) Jacobsen, E. N.; Zhang, W.; Muci, A. R.; Ecker, J. R.; Deng, L. J. *Am. Chem. Soc.* **1991**, *113*, 7063. (b) Larrow, J. F.; Jacobsen, E. N. *J. Am. Chem. Soc.* **1994**, *116*, 12129.

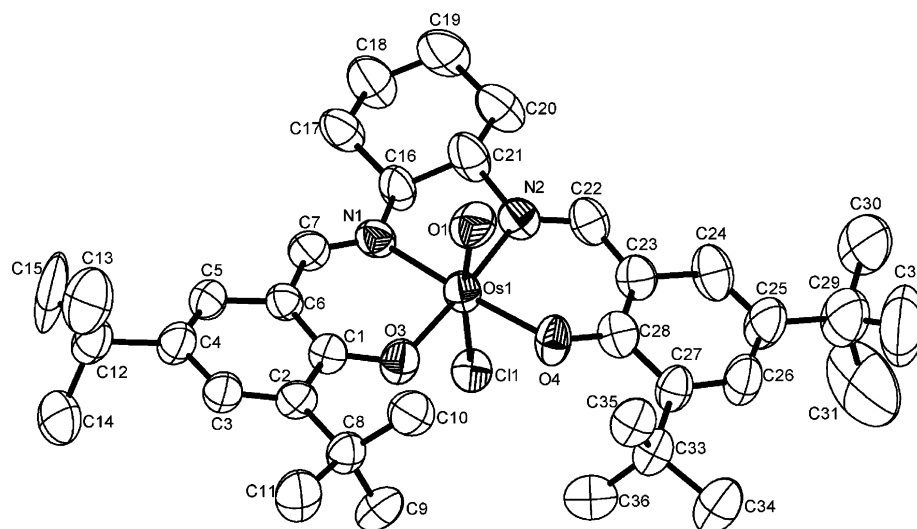


Figure 6. Perspective view of **6**. Hydrogen atoms and solvent molecules have been omitted for clarity. Selected bond lengths (Å) and angles (deg): Os–Cl(1) 2.333(8), Os–O(1) 1.94(2), Os–O(3) 1.996(6), Os–O(4) 1.98(6), Os–N(1) 1.994(8), Os–N(2) 1.983(8), N(1)–C(7) 1.281(11), N(2)–C(22) 1.296(11), Cl(1)–Os–O(1) 170.1(9), Cl(1)–Os–O(3) 93.0(3), Cl(1)–Os–N(2) 87.8(3), O(1)–Os–O(4) 86.8(11), O(1)–Os–N(1) 93.3(3), O(3)–Os–N(2) 176.4(3).¹⁸

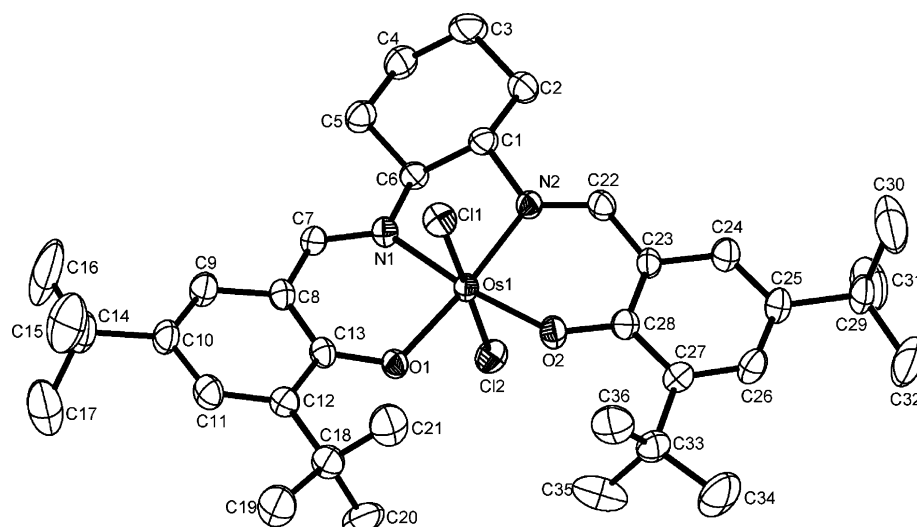


Figure 7. Perspective view of **8**. Hydrogen atoms and solvent molecules have been omitted for clarity. Selected bond lengths (Å) and angles (deg): Os–Cl(1) 2.3495(10), Os–Cl(2) 2.349(1), Os–O(1) 1.976(2), Os–O(2) 1.962(2), Os–N(1) 1.991(3), Os–N(2) 1.997(3), N(1)–C(7) 1.305(4), N(2)–C(22) 1.302(4), Cl(1)–Os–Cl(2) 178.99(3), Cl(1)–Os–O(1) 88.26(8), Cl(1)–Os–N(2) 91.79(9), Cl(2)–Os–O(1) 90.74(8), Cl(2)–Os–N(1) 91.36(9), N(1)–Os–O(1) 91.0(2), N(1)–Os–O(2) 173.7(1).¹⁸

analysis, the enantiomeric excess of the trans product was determined to be 38% ee whereas that of the *cis*-cyclopropane (65% ee) was much higher (Table 6, entry 1). Under similar conditions, cyclopropanation of a series of styrene derivatives bearing either an electron-donating or -withdrawing substituent at the para position with (1*R*,2*R*)-**6** gave the corresponding 2-(*p*-substituted phenyl)-cyclopropanecarboxylic acid ethyl ester products in 49–63% yields and trans/*cis* ratios of up to 2.7:1, along with enantioselectivities of up to 79% ee (entries 2–5). The results are listed in Table 6. A survey of other osmium complexes prepared in this work for similar reactivity showed that neither **5** nor **7** exhibited

any catalytic activity toward alkene cyclopropanation in reaction with styrene and EDA, on the basis of a GC analysis of the reaction mixture.

A series of competition experiments was performed to investigate the product ratios of the cyclopropane esters formed by the reaction of $\text{C}_6\text{H}_5\text{CH}=\text{CH}_2$ versus that of $p\text{-X-C}_6\text{H}_4\text{CH}=\text{CH}_2$ ($\text{X} = \text{MeO}, \text{Me}, \text{Cl}, \text{CF}_3$) with EDA in the presence of **6** (EDA/alkene/**6** = 200:100:1). The ratios of the corresponding cyclopropane esters, defined as the relative rate constants $k_{\text{X}}/k_{\text{H}}$, were determined on the basis of GC analysis. This gave $\log k_{\text{X}}/k_{\text{H}}$ values of 0.525 ($\text{X} = \text{OMe}$), 0.24 ($\text{X} = \text{Me}$), 0.148 ($\text{X} = \text{Cl}$), and -0.40 ($\text{X} = \text{CF}_3$), which suggested that cyclopropanes derived from alkenes substituted with an electron-donating group are more reactive than styrene, whereas those with electron-withdrawing para substituents retard the carbene group transfer process. Fitting (by the least-squares method) the $\log k_{\text{X}}/k_{\text{H}}$ data to the σ^+

(25) During preparation of this manuscript, Nguyen and co-workers reported a ruthenium(II) Schiff-base-catalyzed alkene cyclopropanation procedure. See: (a) Miller, J. A.; Jin, W.; Nguyen, S. T. *Angew. Chem., Int. Ed.* **2002**, *41*, 2953. (b) Miller, J. A.; Hennessy, E. J.; Marshall, W. J.; Scialdone, M. A.; Nguyen S. B. T. *J. Org. Chem.* **2003**, *68*, 7884.

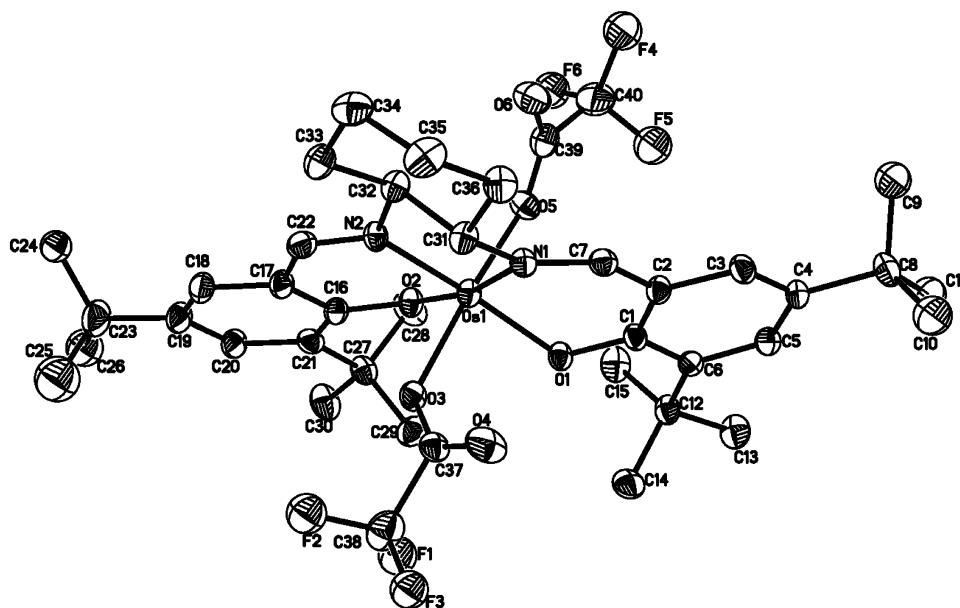


Figure 8. Perspective view of **9**. Hydrogen atoms and solvent molecules have been omitted for clarity. Selected bond lengths (Å) and angles (deg): Os–O(1) 1.954(5), Os–O(2) 1.959(5), Os–O(3) 2.025(6), Os–O(5) 2.041(6), Os–N(1) 2.013(6), Os–N(2) 1.998(6), N(1)–C(7) 1.295(9), N(2)–C(22) 1.317(10), O(1)–Os–O(3) 87.9(2), O(1)–Os–N(1) 89.6(2), O(1)–Os–N(2) 168.3(3), O(2)–Os–O(3) 85.1(2), O(3)–Os–O(5) 167.0(2), N(1)–Os–O(3) 100.3(3), N(1)–Os–O(5) 90.9(3), N(1)–Os–N(2) 81.6(2).¹⁸

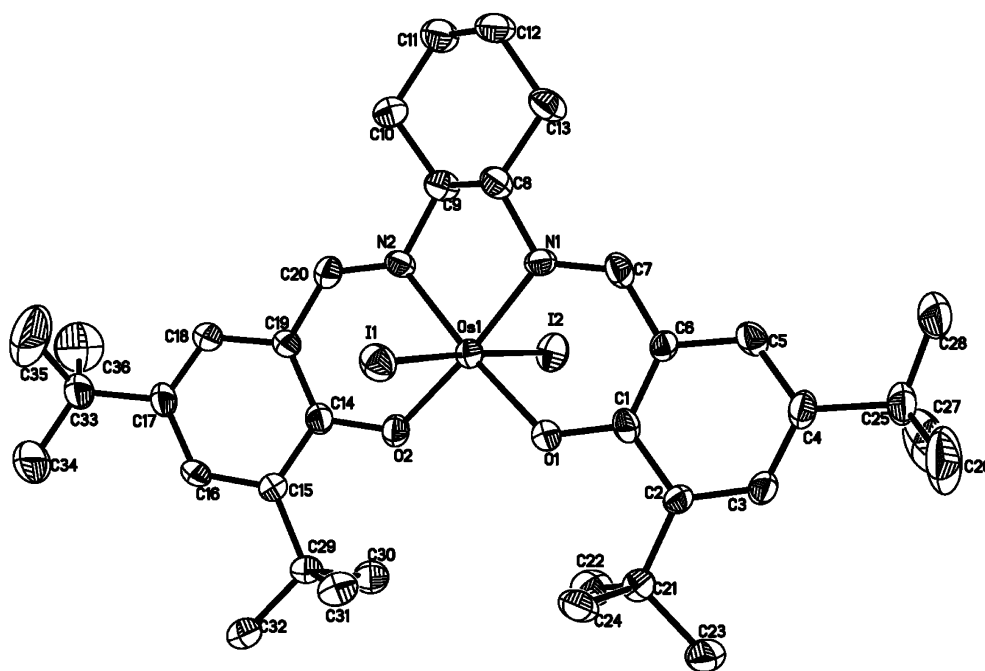


Figure 9. Perspective view of **11**. Hydrogen atoms and solvent molecules have been omitted for clarity. Selected bond lengths (Å) and angles (deg): Os(1)–I(1) 2.6884(6), Os(1)–I(2) 2.6970(6), Os(1)–O(1) 1.976(4), Os(1)–O(2) 1.981(4), Os(1)–N(2) 1.998(5), Os(1)–N(1) 1.999(5), N(1)–C(7) 1.318(7), N(2)–C(20) 1.304(7), O(1)–Os(1)–I(1) 88.23(11), N(2)–Os(1)–I(1) 89.10(13), I(1)–Os(1)–I(2) 177.37(2), O(1)–Os(1)–O(2) 96.70(17), N(2)–Os(1)–N(1) 83.0(2).¹⁸

scale results in reasonable linearity ($R = 0.95$), with a ρ^+ value of -0.66 ± 0.09 (see the Supporting Information).

Although the mechanism is currently unclear, it would not be unreasonable to speculate that the reaction occurs via the initial formation of a metallocarbenoid intermediate that has been shown or proposed to be a reactive species in a number of related ruthenium and osmium systems.^{25–28} Although attempts to isolate such osmium-carbene species proved unsuccessful with either Ph_2CN_2 ²⁹ or EDA as a carbene source, analysis of the reaction mixture obtained from the

treatment of 1 mmol of (1*R*,2*R*)-**6** with EDA (0.2 mmol) in CH_2Cl_2 (5 mL) over an 18 h period at room temperature by FAB mass spectrometry revealed a cluster of peaks with

- (26) (a) Woo, L. K.; Smith, D. A. *Organometallics* **1992**, *11*, 2344. (b) Smith, D. A.; Reynolds, D. N.; Woo, L. K. *J. Am. Chem. Soc.* **1993**, *115*, 2511. (c) Wolf, J. R.; Hamaker, C. G.; Djukic, J.-P.; Kodadek, T.; Woo, L. K. *J. Am. Chem. Soc.* **1995**, *117*, 9194.
(27) For recent reviews, see: (a) Che, C.-M.; Huang, J.-S. *Coord. Chem. Rev.* **2002**, *231*, 151. (b) Lebel, H.; Marcoux, J.-F.; Molinaro, C.; Charette, A. B. *Chem. Rev.* **2003**, *103*, 977. (c) Maas, G. *Chem. Soc. Rev.* **2004**, *33*, 183.

Table 5. Crystal Data and Structure Refinement for Complexes **3a**, **3b**, **6**, **8**, **9**, and **11**¹⁸

	3a ·1.5CHCl ₃	3b	6
formula	C ₃₂ H ₂₆ Br ₄ N ₆ O ₆ Os·1.5CHCl ₃	C ₃₄ H ₂₆ Br ₄ N ₆ O ₂ Os	C ₃₆ H ₅₂ ClN ₂ O ₃ Os
<i>M</i> _R	1279.50	1060.46	786.45
<i>λ</i> [Å]	0.71073	0.71073	0.71073
<i>T</i> [K]	253	294	301
cryst syst	monoclinic	orthorhombic	monoclinic
space group	<i>P</i> 2 ₁ / <i>n</i>	<i>P</i> 2 ₁ 2 ₁ 2 ₁	<i>P</i> 2 ₁ / <i>n</i>
<i>a</i> [Å]	12.574(3)	12.9219(16)	18.688(2)
<i>b</i> [Å]	17.4000(4)	17.563(2)	11.941(1)
<i>c</i> [Å]	19.254(4)	18.195(2)	20.078(2)
<i>α</i> [deg]	90	90	90
<i>β</i> [deg]	104.25(3)	90	94.43(2)
<i>γ</i> [deg]	90	90	90
<i>V</i> [Å ³]	4082.9(16)	4129.3(9)	4467.1(8)
<i>Z</i>	4	4	4
<i>ρ</i> _{calcld} [mg m ^{−3}]	2.082	1.772	1.169
<i>μ</i> (Mo Kα) [mm ^{−1}]	7.384	6.997	2.943
<i>F</i> (000)	2446	2104	1596
index ranges	−13 ≤ <i>h</i> ≤ 14, −19 ≤ <i>k</i> ≤ 19, −21 ≤ <i>l</i> ≤ 21	−16 ≤ <i>h</i> ≤ 16, −22 ≤ <i>k</i> ≤ 22, −23 ≤ <i>l</i> ≤ 16	−22 ≤ <i>h</i> ≤ 22, −13 ≤ <i>k</i> ≤ 12, −23 ≤ <i>l</i> ≤ 23
reflns collected	19063	28099	22173
independent reflns	5921	9438	7467
refinement method	full-matrix least-squares on <i>F</i> ²	full-matrix least-squares on <i>F</i> ²	full-matrix least-squares on <i>F</i> ²
params	312	478	406
GOF	0.94	1.01	1.09
final <i>R</i> indices [<i>I</i> > 2σ(<i>I</i>)] ^a	<i>R</i> ₁ = 0.051, <i>wR</i> ₂ = 0.12	<i>R</i> ₁ = 0.039, <i>wR</i> ₂ = 0.077	<i>R</i> ₁ = 0.059, <i>wR</i> ₂ = 0.2
largest diff. peak:hole [eÅ ^{−3}]	1.346/−1.879	0.940/−0.522	1.308/−1.29
	8	9	11
formula	C ₃₆ H ₅₂ Cl ₂ N ₂ O ₂ Os	C ₄₀ H ₅₄ F ₆ N ₂ O ₆ Os	C ₃₆ H ₅₂ I ₂ N ₂ O ₂ Os
<i>M</i> _R	805.90	963.05	988.80
<i>λ</i> [Å]	0.71073	0.71073	0.71073
<i>T</i> [K]	294	293	301
cryst syst	triclinic	triclinic	orthorhombic
space group	<i>P</i> ₁	<i>P</i> ₁	<i>Pbca</i>
<i>a</i> [Å]	12.1571(11)	12.681(3)	12.522(3)
<i>b</i> [Å]	13.3553(12)	14.074(3)	24.059(5)
<i>c</i> [Å]	13.3721(12)	14.727(3)	26.455(5)
<i>α</i> [deg]	69.7	67.2	90
<i>β</i> [deg]	81.066(2)	72.51	90
<i>γ</i> [deg]	71.178(2)	85.65	90
<i>V</i> [Å ³]	1925.4(3)	2308.3(9)	7970(3)
<i>Z</i>	2	2	8
<i>ρ</i> _{calcld} [mg m ^{−3}]	1.390	1.386	1.648
<i>μ</i> (Mo Kα) [mm ^{−1}]	3.481	2.828	4.779
<i>F</i> (000)	816	972	3840
index ranges	−15 ≤ <i>h</i> ≤ 15, −17 ≤ <i>k</i> ≤ 16, −14 ≤ <i>l</i> ≤ 17	−14 ≤ <i>h</i> ≤ 14, −16 ≤ <i>k</i> ≤ 17, −17 ≤ <i>l</i> ≤ 17	−13 ≤ <i>h</i> ≤ 13, −27 ≤ <i>k</i> ≤ 28, −30 ≤ <i>l</i> ≤ 25
reflns collected	13050	12321	21005
independent refls	8735	6928	5956
refinement method	full-matrix least-squares on <i>F</i> ²	full-matrix least-squares on <i>F</i> ²	full-matrix least-squares on <i>F</i> ²
params	389	484	383
GOF	0.81	1.0	0.50
final <i>R</i> indices [<i>I</i> > 2σ(<i>I</i>)] ^a	<i>R</i> ₁ = 0.045, <i>wR</i> ₂ = 0.11	<i>R</i> ₁ = 0.044, <i>wR</i> ₂ = 0.11	<i>R</i> ₁ = 0.028, <i>wR</i> ₂ = 0.056
largest diff. peak:hole [eÅ ^{−3}]	1.059/−0.933	0.851/−1.617	0.724/−0.584

$$^a R_1 = \sum |F_o| - |F_c| / \sum |F_o|; wR_2 = [\sum w(|F_o| - |F_c|)^2 / \sum w|F_o|^2]^{1/2}.$$

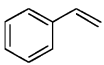
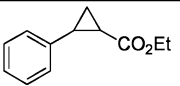
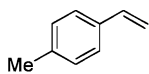
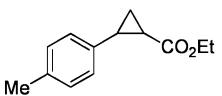
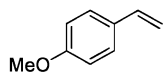
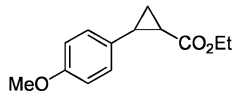
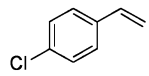
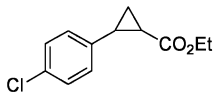
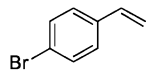
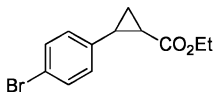
values centered at *m/z* 821 and 907 that match the respective [Os('Bu-salch)(CHCO₂Et)] and [Os('Bu-salch)(CHCO₂Et)₂]

- (28) For works by us, see: (a) Lo, W.-C.; Che, C.-M.; Cheng, K.-F.; Mak, T. C. W. *Chem. Commun.* **1997**, 1205. (b) Che, C.-M.; Huang, J.-S.; Lee, F.-W.; Li, Y.; Lai, T.-S.; Kwong, H.-L.; Teng, P.-F.; Lee, W.-S.; Lo, W.-C.; Peng, S.-M.; Zhou, Z.-Y. *J. Am. Chem. Soc.* **2001**, *123*, 4119. (c) Li, Y.; Huang, J.-S.; Zhou, Z.-Y.; Che, C.-M. *Chem. Commun.* **2003**, 1362; *Chem. Commun.* **2003**, 3052. (d) Zhou, C.-Y.; Chan, P. W. H.; Yu, W.-Y.; Che, C.-M. *Synthesis* **2003**, 9, 1403. (e) Zhang, J.-L.; Chan, P. W. H.; Che, C.-M. *Tetrahedron Lett.* **2003**, *44*, 8733. (f) Zhou, C.-Y.; Yu, W.-Y.; Chan, P. W. H.; Che, C.-M. *J. Org. Chem.* **2004**, *69*, 7072. (g) Li, Y.; Chan, P. W. H.; Zhu, N.-Y.; Che, C.-M.; Kwong, H.-L. *Organometallics* **2004**, *23*, 54.

formulations. Analysis of the FAB mass spectrum also showed cluster peaks with values centered at *m/z* 752, 767, 769, and 786 that could be assigned to [Os('Bu-salch)(OH)], **1a**, **7**, and (1*R*,2*R*)-**6**, respectively. However, FAB mass spectrometric analysis of isolated fractions obtained from purification of the crude reaction mixture by column chromatography showed a marked decrease in the intensity of the signal at *m/z* 821, assigned to [Os('Bu-salch)(CHCO₂-Et)], the complete disappearance of the *m/z* 907 signal

- (29) Miller, J. B. *J. Org. Chem.* **1959**, *24*, 560.

Table 6. [Os^{IV}{(1*R*,2*R*)-(Bu-salch)(OH)(Cl)}] (**6**) Catalyzed Cyclopropanation of Alkenes with EDA^a

entry	alkene	product	yield ^b /(conversion) ^c (%)	<i>trans</i> / <i>cis</i> ^d	<i>trans</i> (% ee) ^e	<i>cis</i> (% ee) ^e
1			50 (37)	2.1:1	38	65
2			49 (25)	2.0:1	31	50
3			51 (27)	2.0:1	22	50
4			67 (16)	2.7:1	35	52
5			43 (23)	2.4:1	37	79

^a Reaction conditions: catalyst/styrene/EDA = 1:100:150; CH₂Cl₂; 40 °C; EDA; addition over 10 h and stirring for 24 h. ^b Isolated yield based on the amount of alkene consumed. ^c Determined by GC analysis with tribromobenzene as an internal standard. ^d Determined by analytical GC column. ^e Determined by HPLC using chiral OJ column. In addition to the cyclopropane adduct, diethyl fumarate and diethyl maleate were obtained as side products, but the yields of these latter compounds were not determined.

assigned to [Os(Bu-salch)(CHCO₂Et)₂], and the appearance of a cluster of peaks centered at *m/z* 1522 that could be assigned to [μ-O-{Os(Bu-salch)O}₂]. In addition, the formation of diethyl fumarate was detected by ¹H NMR spectroscopy in monitoring the reaction of 19 μmol of (1*R*,2*R*)-**6** with EDA (1.2 μmol) in CDCl₃ (1 mL) over a 10 h period at room temperature (see the Supporting Information). Thus, the inability to isolate the osmium-carbenoid species in the pure form could be due to its instability; similar observations in related ruthenium and osmium systems have previously been reported.^{25–28}

Conclusion

In this article, we describe the synthesis of *trans*-dioxoosmium(VI) containing sterically bulky Schiff-base complexes. The reactions of **1a** with PPh₃ were shown to give a complex mixture of products, but the analogous reaction of **1b** with PPh₃ furnished **2**. In addition, reactions of **1b** with arylamines gave the bis(amido)osmium(IV) Schiff-base complexes **3a** and **3b** in moderate yields. Reaction of **1a** with *p*-nitroaniline is the only example where the μ-oxo-bridged Os(IV) Schiff-base complex **4** was preferentially furnished. With hydrazine compounds, the expected bis(hydrazido)osmium(IV) Schiff-base complexes were not obtained. These reactions preferentially furnish **5**, **6**, and **7** in good yields. Reaction of **1a** with either thionyl chloride, trifluoroacetic acid, bromine, or iodine under reducing conditions, on the other hand, gave the expected Os(IV) complexes **8–11** in good yields. ¹H NMR spectroscopy and X-ray crystallographic analyses reveal that the ligands in these complexes form a chiral environment around the metal center. Upon UV irradiation, (1*S*,2*S*)-**1** was demonstrated to undergo light-induced epoxidation with a series of alkenes in moderate yields, albeit with no enantio-

selectivity. When treated with EDA, (1*R*,2*R*)-**6** was shown to catalyze alkene cyclopropanation with moderate *trans* selectivity and moderate to good enantioselectivities. Our studies lead us to speculate that EDA decomposition in the presence of (1*R*,2*R*)-**6** gives a metallocarbenoid intermediate that undergoes carbene transfer via a carboradical species that cyclizes to give the cyclopropane. Product formation was shown to occur more quickly for reactions derived from alkenes substituted with an electron-donating group compared to those derived from electron-withdrawing substituted alkenes.

Experimental Section

General Considerations. 3,5-Di-*tert*-butyl-2-hydroxybenzaldehyde (99%; Aldrich), *trans*-(±)-(1*R*,2*R*)- and (1*S*,2*S*)-1,2-cyclohexanediamine (99%; Aldrich), OsO₄ (99.8%; Aldrich), 4-nitroaniline (99%+; Aldrich), 4-chloroaniline (98%; Aldrich), and 1,1-diphenylhydrazine hydrochloride (97%; Aldrich) were all purchased and used as received. All of the solvents used were of AR grade. K₂[Os^{VI}O₂(OH)₄] was prepared following the literature procedure.³⁰ Bis(3,5-di-*tert*-butylsalicylidene)-1,2-cyclohexane-diamine (H₂tBu-salch) and bis(3,5-dibromosalicylidene)-1,2-cyclohexane-diamine (H₂Br-salch) were prepared from the reaction of 3,5-di-*tert*-butyl-2-hydroxybenzaldehyde or 3,5-dibromo-2-hydroxybenzaldehyde with 1,2-cyclohexanediamine in ethanol (2:1), respectively.

Instrumentation. ¹H NMR spectra were recorded on either a Bruker DPX 300 or a Bruker DPX 400 spectrometer at 300 or 400 MHz. The chemical shifts (δ, ppm) were reported relative to tetramethylsilane (TMS). IR spectra were measured on a Bio-Rad FT-IR spectrometer. UV–vis spectra were recorded on a Hewlett-Packard 8452A Diode Array spectrophotometer. FAB mass spectra were measured on a Finnigan MAT 95 mass spectrometer using 3-nitrobenzyl alcohol as the matrix. HPLC measurements were

(30) Malin, J. M. *Inorg. Synth.* **1980**, 20, 61.

carried out on a HP 1050 Series HPLC. Cyclic voltammetry was performed with a Bioanalytical Systems (BAS) model 100 B/W electrochemical analyzer. A conventional two-compartment electrochemical cell was used. The glassy carbon electrode was polished with 0.05 mm alumina on a microcloth, sonicated for 5 min in deionized water, and rinsed with MeCN before use. An Ag/AgNO₃ (0.1 M in MeCN) electrode was used as the reference electrode. All of the solutions were degassed with argon before the experiments. $E_{1/2}$ values were taken from the average of the cathodic and anodic peak potentials for the oxidative and reductive waves. The $E_{1/2}$ value of the ferrocenium/ferrocene couple (Cp₂Fe⁺⁰) measured in the same solution was used as an internal reference.

General Procedure for the Synthesis of Dioxosmium(VI)-(Schiff-Base) Complexes 1. A few drops of HCl (2M) was slowly added to a mixture of K₂[Os^{VI}O₂(OH)₄] (100 mg, 0.27 mmol) and either H₂Br-salch or H₂tBu-salch (100 mg, 0.18 mmol) in MeOH (25 mL). The mixture was then stirred for several minutes. Upon the addition of 2,6-lutidine (0.1 mL), an orange solid was observed to slowly precipitate. The crude product was recrystallized by the diffusion of Et₂O into a solution of CH₂Cl₂.

[Os^{VI}(Bu-salch)O₂] (1a). Yield: 70%. Anal. Calcd for C₃₆H₅₂N₂O₄-Os: C, 56.37; H, 3.65; N, 6.38. Found: C, 56.20; H, 3.89; N, 7.01. ¹H NMR (300 MHz, CDCl₃): δ 8.38 (s, 2H), 7.66 (d, 2H, $J = 2.6$ Hz), 7.14 (d, 2H, $J = 2.6$ Hz), 3.98 (m, 2H), 3.81 (m, 2H), 2.04 (m, 2H), 1.73 (m, 2H), 1.58 (s, 18H), 1.48 (m, 2H), 1.32 (s, 18H). IR (KBr pellet, cm⁻¹): 1636, 1533, $\nu_{\text{as(Os=O)}}$ 833. FAB MS: m/z 767 [M]⁺, 751 [M - O]⁺, 735 [M - 2O]⁺.

[Os^{VI}(Br-salch)O₂] (1b). Yield: 65%. Anal. Calcd for C₂₀H₁₆-Br₄N₂O₄Os: C, 27.99; H, 1.88; N, 3.26. Found: C, 27.50; H, 1.92; N, 3.10. IR (KBr pellet, cm⁻¹): 1642, 1581, $\nu_{\text{as(Os=O)}}$ 841. FAB MS: m/z 858 [M]⁺, 842 [M - O]⁺, 826 [M - 2O]⁺.

[Os^{III}(Br-salch)(OPPh₃)₂] (2). A solution of MeCN (20 mL) containing **1b** (86 mg, 0.1 mmol) and PPh₃ (262 mg, 1 mmol) was stirred for 24 h. The reaction mixture was filtered and evaporated to dryness. The brown solid obtained was recrystallized from a solution of CH₂Cl₂ and Et₂O to give the title compound. Yield: 70%. IR (Nujol, cm⁻¹): $\nu_{\text{(P-Ph)}}$ 1420, $\nu_{\text{(P-Ph)}}$ 1155, $\nu_{\text{(O=P)}}$ 1121, $\nu_{\text{(P-Ph)}}$ 1066. FAB MS: m/z 1382 [M + H]⁺.

General Procedure for the Synthesis of Bis(arylamido)-osmium(IV) Complexes 3a, 3b, and 4. To a solution of **1** (40 mg, 0.05 mmol) and arylamine (128 mg, 1 mmol) in CH₂Cl₂ (20 mL) was added one drop of N₂H₄·H₂O. The mixture was stirred for 24 h at room temperature. The resulting green solution was evaporated to dryness. The solid was dissolved in CH₂Cl₂, which was purified on a silica gel column with CH₂Cl₂ as an eluent. The second green band was eluted with CH₂Cl₂/acetone (2:1 v/v), collected, and evaporated to dryness to give the title compound as a green solid.

[Os^{IV}(Br-salch)(p-NO₂C₆H₄NH)₂] (3a).¹⁸ Yield: 30%. Anal. Calcd for C₃₂H₂₆Br₄N₆O₆Os·2CHCl₃: C, 32.85; H, 2.27; N, 6.76. Found: C, 33.01; H, 1.90; N, 6.90. ¹H NMR (300 MHz, acetone-*d*₆): δ 9.38 (s, 2H), 8.02 (m, 4H), 7.86 (d, 2H, $J = 2.4$ Hz), 7.53 (d, 2H, $J = 2.4$ Hz), 6.92 (m, 4H), 3.92 (m, 2H), 2.24–0.86 (m, 8H). IR (Nujol, cm⁻¹): ν_{NH} 3290. FAB MS: m/z 1101 [M + H]⁺, 963 [M - p-NO₂C₆H₄NH]⁺, 826 [M - 2(p-NO₂C₆H₄NH)]⁺.

[Os^{IV}(Br-salch)(p-CNC₆H₄NH)₂] (3b).¹⁸ Yield: 30%. Anal. Calcd for C₃₄H₂₆Br₄N₆O₆Os·2.5CH₂Cl₂: C, 34.44; H, 2.45; N, 6.60. Found: C, 34.53; H, 2.24; N, 6.69. ¹H NMR (300 MHz, acetone-*d*₆): δ 9.23 (s, 2H), 7.77 (d, 2H, $J = 2.5$ Hz), 7.52 (d, 2H, $J = 2.5$ Hz), 7.46 (d, 4H, $J = 9.0$ Hz), 7.08 (m, 4H), 4.00 (m, 2H), 3.31 (m, 2H), 2.19 (m, 4H), 1.68 (m, 2H). IR (Nujol, cm⁻¹): ν_{NH} 3296, $\nu_{\text{C≡N}}$ 2207. FAB MS: m/z 1060 [M]⁺, 943 [M - p-CNC₆H₄NH]⁺, 826 [M - 2(p-CNC₆H₄NH)]⁺.

[μ-O-{[Os^{IV}(Bu-salch)(p-NO₂C₆H₄NH)]₂} (4). Yield: 50%. Anal. Calcd for C₈₄H₁₁₄N₈O₉Os₂·2(CH₃)₂CO: C, 57.61; H, 6.77; N, 5.97. Found: C, 57.93; H, 6.52; N, 5.82. IR (Nujol, cm⁻¹): ν_{NH} 3287. FAB MS: m/z 1761 [M + H]⁺, 1624 [M - p-NO₂C₆H₄NH]⁺, 1487 [M - 2(p-NO₂C₆H₄NH)]⁺, 889 [M - p-NO₂C₆H₄NH - {Os(Bu-salch)}]⁺, 751 [M - 2(p-NO₂C₆H₄NH) - {Os(Bu-salch)}]⁺, 735 [M - 2(p-NO₂C₆H₄NH) - {Os(Bu-salch)} - O]⁺.

[Os^{III}(Br-salch)(N₂)(H₂O)] (5). To a DMF (10 mL) solution containing **1b** (20 mg) was added several drops of hydrazine monohydrate. The reaction mixture was stirred at room temperature for 10 min, quenched with water (40 mL), filtered, and concentrated in vacuo to afford a light green solid. The crude product was recrystallized by slow diffusion of Et₂O into a CHCl₃ solution. Yield: 50%. Anal. Calcd for C₂₀H₁₈Br₄N₄O₃Os·2CHCl₃: C, 23.78; H, 1.81; N, 5.04. Found: C, 23.62; H, 2.20; N, 5.19. IR (KBr pellet, cm⁻¹): $\nu_{\text{N=N}}$ 2017, $\nu_{\text{C=N}}$ 1638.

[Os^{IV}(Bu-salch)(OH)(Cl)] (6).¹⁸ A solution of 1,1-diphenylhydrazine hydrochloride (220 mg, 1 mmol) and KOH (90 mg, 1.4 mmol) in CH₂Cl₂ (20 mL) was stirred for 1 h. Complex **1a** (40 mg, 0.05 mmol) was added to the resulting brown mixture, and the reaction was stirred for 1 further day at room temperature. The brown solution was observed to turn green after evaporation to dryness. The green residue was loaded on a silica gel column, which was first eluted with CH₂Cl₂/*n*-hexane (1:1 v/v) to remove the brown band. The green band was eluted with 3% MeOH in CH₂Cl₂ to give **6**. Yield: 80%. Anal. Calcd for C₃₆H₅₃ClN₂O₃Os·0.5C₆H₁₄: C, 56.40; H, 7.28; N, 3.37. Found: C, 56.07; H, 7.26; N, 3.24. ¹H NMR (300 MHz, CDCl₃): δ 10.58 (d, 1H, $J = 2.4$ Hz), 10.37 (d, 1H, $J = 2.4$ Hz), 9.38 (s, 1H), 8.30 (s, 1H), 6.99 (d, 1H, $J = 2.5$ Hz), 6.81 (d, 1H, $J = 2.5$ Hz), 2.86 (m, 1H), 2.61 (m, 1H), 2.32 (s, 9H), 2.29 (s, 9H), 1.27 (m, 2H), 0.85 (m, 6H), 0.57 (s, 9H), 0.39 (s, 9H). IR (Nujol, cm⁻¹): ν_{OH} 3533. FAB MS: m/z 788 [M + H]⁺, 771 [M - OH]⁺, 753 [M - Cl]⁺, 735 [M - Cl - OH]⁺.

[Os^{IV}(Bu-salch)(OH)₂] (7). This compound was prepared following the procedure of **4** but with NEt₃ as the base. Yield: 60%. Anal. Calcd for C₃₆H₅₄N₂O₄Os: C, 56.22; H, 7.08; N, 3.64. Found: C, 56.77; H, 7.37; N, 3.56. ¹H NMR (400 MHz, CDCl₃): δ 8.30 (d, 2H, $J = 1.9$ Hz), 6.41 (d, 2H, $J = 2.4$ Hz), 5.35 (s, 2H), 3.17 (m, 2H), 1.91 (s, 18H), 1.69 (m, 2H), 1.28 (s, 18H), 1.12 (m, 4H), -0.07 (m, 2H). IR (KBr pellet, cm⁻¹): ν_{OH} 3557, 1595, 1524. FAB MS: m/z 769 [M]⁺, 752 [M - OH]⁺, 735 [M - 2OH]⁺.

[Os^{IV}(Bu-salch)Cl₂] (8).¹⁸ Complex **1a** (100 mg, 0.13 mmol) was dissolved in CH₂Cl₂ (15 mL), and one drop of N₂H₄·H₂O was subsequently added. Excess SOCl₂ (0.1 mL) was slowly added, and the reaction mixture was stirred overnight. The resulting green solution was evaporated to dryness. The residue was loaded on an alumina column with CH₂Cl₂ as an eluent. The green band was collected and concentrated to 1–2 mL. The addition of *n*-hexane gave a green solid. Crystals of **7** were obtained by slow diffusion of Et₂O into a CH₂Cl₂ solution. Yield: 70%. Anal. Calcd for C₃₆H₅₂N₂Cl₂O₂Os: C, 53.65; H, 6.50; N, 3.48. Found: C, 54.02; H, 6.32; N, 3.88. ¹H NMR (300 MHz, CDCl₃): δ 16.44 (s, 2H), 12.43 (d, 2H, $J = 2.1$ Hz), 8.04 (d, 2H, $J = 2.4$ Hz), 4.94 (m, 2H), 2.37 (s, 18H), 1.99 (m, 2H), 0.15 (m, 4H), -0.21 (s, 18H), -1.27 (m, 2H). IR (KBr pellet, cm⁻¹): 1584. FAB MS: m/z 807 [M + H]⁺, 772 [M - Cl]⁺, 735 [M - 2Cl]⁺.

[Os^{IV}(Bu-salch)(CF₃CO₂)₂] (9).¹⁸ To a solution of **1a** (78 mg, 0.1 mmol) was added CF₃CO₂H (16 mL) and PPh₃ (150 mg) in tetrahydrofuran (THF; 20 mL). The reaction mixture was heated for 1 h. Upon cooling to room temperature and removal of the solvent, the residue was dissolved in CH₂Cl₂ and purified by silica gel chromatography with CH₂Cl₂ as an eluent. The first band was collected and evaporated to dryness to give the title compound as

a green solid. Yield: 40%. Anal. Calcd for $C_{40}H_{54}F_6N_2O_6Os \cdot 0.25C_6H_{14}$: C, 50.62; H, 5.89; N, 2.85. Found: C, 50.74; H, 5.75; N, 2.64. 1H NMR (300 MHz, $CDCl_3$): δ 14.07 (s, 2H), 10.40 (d, 2H, $J = 2.4$ Hz), 7.56 (d, 2H, $J = 2.4$ Hz), 6.31 (m, 2H), 2.31 (m, 2H), 1.96 (s, 18H), 0.70 (m, 2H), 0.42 (m, 2H), 0.34 (s, 18H), -0.01 (m, 2H). IR (Nujol, cm^{-1}): $\nu_{C=O}$ 1711. FAB MS: m/z 963 $[M]^+$, 850 $[M - CF_3CO_2]^+$, 735 $[M - 2(CF_3CO_2)]^+$.

[Os^{IV}(Bu-salch)Br₂] (10). To a solution of **1a** (78 mg, 0.1 mmol) in anhydrous THF (20 mL) was added 2 drops of $N_2H_4 \cdot H_2O$. After the reaction mixture was stirred for 20 min at room temperature, two drops of Br_2 solution was added. The reaction was stirred for 1 further day. The resultant green solution obtained was evaporated to dryness and loaded on a silica gel column, which was eluted with CH_2Cl_2 to isolate the green band and furnish the title compound as a green solid. Yield: 50%. Anal. Calcd for $C_{36}H_{52}N_2O_2Br_2Os \cdot 0.5CH_2Cl_2 \cdot 0.25C_6H_{14}$: C, 47.61; H, 5.95; N, 2.92. Found: C, 47.63; H, 6.09; N, 2.92. 1H NMR (400 MHz, $CDCl_3$): δ 19.31 (s, 2H), 13.07 (s, 2H), 8.44 (s, 2H), 6.49, 2.46 (s, 18H), 2.00 (m, 2H), 0.08 (m, 2H), -0.27 (s, 20H), -1.49 (m, 2H). IR (KBr pellet, cm^{-1}) 1583. FAB MS: m/z 894 $[M]^+$, 815 $[M - Br]^+$, 735 $[M - 2 Br]^+$.

Synthesis of [Os^{IV}(Bu-salch)I₂] (11).¹⁸ To a solution of **1a** (78 mg, 0.1 mmol) in anhydrous THF (20 mL) was added 2 drops of $N_2H_4 \cdot H_2O$. After the reaction mixture was stirred for 20 min at room temperature, I_2 (100 mg) was added. The reaction was stirred for 1 further day. The resultant brown solution was evaporated to dryness and loaded onto a silica gel column. Excess I_2 was removed by eluting with *n*-hexane, and CH_2Cl_2 was used as an eluent to isolate the brown band and furnish the title compound as a brown solid. Yield 80%. Anal. Calcd for $C_{36}H_{52}N_2O_2I_2Os \cdot 0.4C_6H_{14}$: C, 44.97; H, 5.67; N, 2.73. Found: C, 44.91; H, 5.72; N, 2.61. 1H NMR (400 MHz, $CDCl_3$): δ 22.15 (s, 2H), 13.71 (s, 2H), 8.81 (s, 2H), 8.35 (m, 2H), 2.56 (s, 18H), 1.99 (d, $J = 3.0$ Hz, 2H), 1.49 (m, 2H), 0.31 (s, 20H), -1.89 (m, 2H). IR (KBr pellet, cm^{-1}) 1578. FAB MS: m/z 990 $[M]^+$, 863 $[M - I]^+$, 735 $[M - 2I]^+$.

X-ray Crystallography. Crystals of **3a** and **3b** were obtained by slow diffusion of $CHCl_3$ into acetone solutions of either **3a** or **3b**, whereas those of **6**, **8**, and **9** were obtained by slow diffusion of *n*-hexane into $CHCl_3$ solutions of either **6**, **8**, or **9**, respectively, and those of **11** was obtained by slow diffusion of Et_2O into a CH_2Cl_2 solution containing **11**.¹⁸ For **3b** and **8**, the data were collected on a Bruker SMART CCD diffractometer by employing a crystal of the dimensions $0.22 \times 0.14 \times 0.12$ mm³ at 294 K and $0.20 \times 0.14 \times 0.12$ mm³ at 294 K, respectively. The structures were refined by full-matrix least squares using the SHELXL-97³¹ program. For the other four complexes, data collection was made on a MAR diffractometer by using a crystal of the dimensions of $0.40 \times 0.20 \times 0.10$ (**3a**·1.5 $CHCl_3$, at 253 K), $0.50 \times 0.20 \times 0.20$ (**6**, at 301 K), $0.50 \times 0.30 \times 0.25$ mm³ (**9**, at 293 K), and $0.50 \times 0.12 \times 0.08$ mm (**11**, at 301K). The images were interpreted and the intensities integrated by using the program DENZO.³² The structures were solved by direct methods by employing the SHELXS-97³³

program on a PC. In all cases, graphite monochromatized Mo K α radiation ($\lambda = 0.71073$ Å) was used.

Procedure for Photoinduced Oxidation of Alkenes by [Os^{VI}{1*S*,2*S*}(Bu-salch)O₂] (1a). A CH_2Cl_2 /MeCN (2:1 v/v, 150 mL) solution containing (1*S*,2*S*)-**1a** (65 μ mol) and alkene (6.5 mmol) was placed in a photochemical reactor (Rayonet RPR-100) and irradiated with an array of 16 low-pressure mercury arc lamps (RPR-2537) for 24 h. After evaporation of the reaction mixture to dryness, product yields were determined by GC using an analytic column with tribromobenzene as an internal standard. IR and 1H NMR spectroscopy were used to determine the organic and inorganic products obtained.

Procedure for [Os^{IV}{1*R*,2*R*}(Bu-salch)(OH)(Cl)] (6) Catalyzed Cyclopropanation of Alkenes with EDA. A solution of EDA (1.5 mmol) in CH_2Cl_2 (5 mL) was added dropwise to a solution of alkene (1 mmol) and (1*R*,2*R*)-**5** (0.01 mmol) in CH_2Cl_2 (5 mL) over a 10 h period at room temperature under an argon atmosphere. The mixture was then stirred for an additional 24 h. After purification by flash chromatography on a short column of silica gel, substrate conversion and the ratio of *trans*- to *cis*-cyclopropyl esters were determined by GC using an analytic column with tribromobenzene as an internal standard. Further purification of the cyclopropyl esters was carried out by column chromatography on silica gel with *n*-hexane/EtOAc (20:1 v/v) as an eluent.

Competitive Cyclopropanations Catalyzed by (1*R*,2*R*)-6. In a typical experiment, equimolar amounts of each alkene (1.5 mmol) and (1*R*,2*R*)-**6** (0.015 mmol) were dissolved in CH_2Cl_2 (2 mL) at room temperature. A solution of EDA (0.3 mmol) in CH_2Cl_2 (1 mL) was added over a 6 h period. The cyclopropane esters obtained were analyzed by GC spectroscopy.

Acknowledgment. We thank Dr. Po Hung Ko and Siu-Chung Chan for contributions made to the synthesis and photochemistry of the dioxoosmium(VI) complexes reported in this paper. This work is supported by the Area of Excellence Scheme (AoE/P-10-01) established under the University Grants Committee, HKSAR, the Hong Kong Research Grants Council (HKU7384/02P), HKSAR, and The University of Hong Kong (University Development Fund). P.W.H.C. wishes to thank The University of Hong Kong (Small Project Funding Program) for funding.

Supporting Information Available: Circular dichroism spectra of (1*R*,2*R*)- and (1*S*,2*S*)-**1a**, including an 1H NMR spectrum of **1a**; 1H NMR spectrum of **7**; UV-vis spectra for **1a**, **3a**, and **6–11**; cyclic voltammograms of **3a**, **3b**, and **6–11**; data and a plot of linear-free-energy correlation of $\log k_X/k_H$ versus σ^+ for reactions of (1*R*,2*R*)-**6** with a series of para-substituted styrenes at 298 K; FAB mass spectra of UV irradiated (1*S*,2*S*)-**1a**; full experimental details and spectroscopic analysis for the reaction of (1*R*,2*R*)-**6** with EDA; and crystallographic data in CIF format for **3a**, **3b**, **6**, **8**, **9**, and **11**. This material is available free of charge via the Internet at <http://pubs.acs.org>.

IC0481935

(31) Sheldrick, G. M. *SHELXL97. Programs for Crystal Structure Analysis*, release 97-2; University of Goettingen: Goettingen, Germany, 1997.

(32) Otwinowski, Z.; Minor, W. "Processing of X-ray Diffraction Data Collected in Oscillation Mode". *Methods in Enzymology, Macromolecular Crystallography, Part A*; Carter, C. W., Sweet, R. M., Jr., Eds.; Academic Press: New York, 1997; Vol. 276, pp 307–326.

(33) Sheldrick, G. M. *SHELXS97. Programs for Crystal Structure Analysis*, release 97-2; University of Goettingen: Goettingen, Germany, 1997.